

Climate Change Impacts on Net Ecosystem Productivity in a Subtropical Shrubland of Northwestern México

Vivian S. Verduzco^{1,2}, Enrique R. Vivoni^{2,3*}, Enrico A. Yépez¹, Julio C. Rodríguez⁴, Christopher J. Watts⁵, Tonantzin Tarin^{1,6}, Jaime Garatuza-Payán¹, Agustín Robles-Morua¹ and Valeriy Y. Ivanov⁷

¹ Departamento de Ciencias del Agua y Medio Ambiente. Instituto Tecnológico de Sonora. Ciudad Obregón, Sonora, México, 85000

² School of Earth and Space Exploration. Arizona State University. Tempe, Arizona, USA, 85287

³ School of Sustainable Engineering and the Built Environment. Arizona State University. Tempe, Arizona, USA, 85287

⁴ Departamento de Agricultura y Ganadería. Universidad de Sonora. Hermosillo, Sonora, México, 83000

⁵ Departamento de Física. Universidad de Sonora. Hermosillo, Sonora, México, 83000

⁶ School of Life Sciences. University of Technology Sydney. Sydney, Australia, 2007

⁷ Department of Civil and Environmental Engineering. University of Michigan. Ann Arbor, Michigan, USA, 48109

*Corresponding author: Dr. Enrique R. Vivoni, e-mail: vivoni@asu.edu

- Model simulation accurately captured the seasonality of vegetation activity.
- Net ecosystem productivity decreased under reduced summer rainfall and increased temperature scenarios.
- Elevated CO₂ scenarios offset the negative impacts of meteorological conditions.

Paper 2017JG004361 Revised for

Journal of Geophysical Research- Biogeosciences

February 7, 2018

This is the author manuscript accepted for publication and has undergone full peer review but has not been through the copyediting, typesetting, pagination and proofreading process, which may lead to differences between this version and the Version of Record. Please cite this article as doi: [10.1002/2017JG004361](https://doi.org/10.1002/2017JG004361)

1 **Abstract**

2 The sensitivity of semiarid ecosystems to climate change is not well understood due to
3 competing effects of soil and plant-mediated carbon fluxes. Limited observations of net
4 ecosystem productivity (NEP) under rising air temperature and CO₂ and altered precipitation
5 regimes also hinder climate change assessments. A promising avenue for addressing this
6 challenge is through the application of numerical models. In this work, we combine a
7 mechanistic ecohydrological model and a soil carbon model to simulate soil and plant processes
8 in a subtropical shrubland of northwest México. Due to the influence of the North American
9 monsoon, the site exhibits net carbon losses early in the summer and net carbon gains during the
10 photosynthetically-active season. After building confidence in the simulations through
11 comparisons with eddy covariance flux data, we conduct a series of climate change experiments
12 for near-future (2030-2045) scenarios that test the impact of meteorological changes and CO₂
13 fertilization relative to historical conditions (1990-2005). Results indicate that reductions in NEP
14 arising from warmer conditions are effectively offset by gains in NEP due to the impact of higher
15 CO₂ on water use efficiency. For cases with higher summer rainfall and CO₂ fertilization, climate
16 change impacts lead to an increase of ~25% in NEP relative to historical conditions (mean of 66
17 gC m⁻²). Net primary production and soil respiration derived from decomposition are shown to
18 be important processes that interact to control NEP and, given the role of semiarid ecosystems in
19 the global carbon budget, deserve attention in future simulation efforts of ecosystem fluxes.

20 **Keywords:** ecohydrology; eddy covariance; carbon fluxes; modeling; climate change; North
21 American monsoon.

22 **1. Introduction**

23 Although the carbon sink strength of semiarid ecosystems is still under debate (Xiao et
24 al., 2011), recent studies have recognized that these areas have a dominant role, stronger than
25 other biogeographic regions, in regulating the intra- and inter-annual variability of the global
26 carbon cycle (Ahlström et al., 2015; Poulter et al., 2014). A transition to more arid conditions
27 (e.g. increasing temperatures and prolonged drought spells) in these regions (Pachauri et al.,
28 2014; Seager et al., 2007) will have implications on the productivity of semiarid ecosystems.
29 This is the case for most of the North American monsoon (NAM) region, which comprises
30 semiarid areas in the southwestern United States and northwestern México (Douglas et al., 1993;
31 Vivoni et al., 2008). The NAM system is a pronounced increase in precipitation during the warm
32 season (July-September) leading to increased biological activity (Flato et al., 2013; Forzieri et
33 al., 2014). Remote sensing analyses have quantified the spatial and temporal variability of
34 vegetation greening during the NAM (e.g. Tang et al., 2012; Watts et al., 2007). However,
35 ecosystem processes regulating the carbon cycling are not understood well enough to anticipate
36 the implications of climate change on the net carbon balance of these semiarid ecosystems.

37 The eddy covariance (EC) technique has become a useful approach for measuring water,
38 energy and carbon fluxes at the ecosystem level (Baldocchi et al., 2001), with several studies
39 conducted in different ecosystems in the NAM region (e.g. Anderson & Vivoni, 2016; Méndez-
40 Barroso et al., 2014; Pérez-Ruiz et al., 2010; Scott et al., 2010, 2015; Yépez et al., 2007). By
41 quantifying carbon dioxide (CO₂) exchanges between ecosystems and the overlying atmosphere
42 (Loescher et al., 2003), net ecosystem productivity (NEP) can be measured via the EC method as
43 a degree of the metabolic activity of a terrestrial ecosystem. Furthermore, traditional flux
44 partitioning models have been applied to estimate NEP components, gross primary productivity

45 (GPP) and ecosystem respiration (R_{ECO}) (Reichstein et al., 2005, Stoy et al., 2006). Since NEP
46 consists of the difference between GPP and R_{ECO} , its response to hydrometeorological conditions
47 has been difficult to identify (Nayak et al., 2015; Scott et al., 2015; Biederman et al., 2016). This
48 is primarily due to the differential sensitivity of GPP and R_{ECO} to changes in temperature and
49 precipitation (e.g. Euskirchen et al., 2014; Shi et al., 2014). As a result, semiarid ecosystem
50 responses to climate change remain highly uncertain. On the one hand, GPP may be reduced by
51 warming via plant heat stress (Sage & Kubien, 2007) and via stomatal closure from increased
52 evaporative demand and reductions of soil water content (Seneviratne et al., 2010; Williams et
53 al., 2013) affecting vegetation productivity (Novick et al., 2016). For instance, Biederman et al.
54 (2017) found that warm temperatures have a negative effect on NEP in semiarid ecosystems of
55 southwestern North America. Stomata respond to transpiration rates in a process known as the
56 apparent ‘feed-forward response’, implying that transpiration strongly decreases at high vapor
57 pressure deficit, particularly during periods of water stress (Duurmsa et al., 2014; Novick et al.,
58 2016). When stomata close in this manner, carbon assimilation and GPP decrease, thus reducing
59 NEP. Photosynthetic enhancements due to rising CO_2 atmospheric concentrations (Smith et al.,
60 2000) and the lengthening of the growing season (Kunkel, 2016), however, may increase GPP.
61 These changes are known to affect ecosystem water use efficiency ($\text{WUE} = \text{GPP} /$
62 $\text{evapotranspiration (ET)}$), a measure of the sensitivity of photosynthesis rates to changes in
63 hydroclimatic conditions (Yang et al., 2016). In addition, changes in rainfall timing, intensity and
64 distribution are also important factors affecting NEP, though the net effect or directionality are
65 unclear (Allard et al., 2008; Gherardi & Sala, 2015; Heisler-White et al., 2008; Miranda et al.,
66 2011; Robertson et al., 2009; Rohr et al., 2013; Ross et al., 2012; Xie et al., 2015).

67 Similarly, the effects of climate change on R_{ECO} in semiarid ecosystems are uncertain due
68 to complex dynamics occurring during periods of water availability (Collins et al., 2014; Fan et
69 al., 2012). R_{ECO} integrates plant (autotrophic) and microbial (heterotrophic) processes that are
70 coupled (Sacks et al., 2007; Verduzco et al., 2015) and has been shown to either increase,
71 decrease or remain unchanged under warming conditions (Arnone et al., 2008; Lenton &
72 Huntingford, 2003; Luo et al., 2001; Zhou et al., 2007). R_{ECO} is also highly variable under
73 different precipitation conditions (Cable et al., 2008; Harper et al., 2005; Thomey et al., 2011).
74 Some studies have found that warming can substantially increase cellular metabolic maintenance
75 (e.g. Amthor, 1984; Ryan, 1991), which in turn affects autotrophic respiration (R_a). Although
76 studies have shown that plants can acclimate to increasing temperatures (Slot and Kitajima,
77 2015), it is still unknown the degree of and time to acclimation for different plant functional
78 types (Drake et al., 2015; Yamori et al., 2014). Furthermore, heterotrophic respiration has been
79 observed to respond positively to temperature (Lloyd & Taylor, 1994), but its sensitivity has
80 been related to limiting factors such as substrate availability and quality, which are coupled to
81 primary productivity (Sponseller, 2007; Zhou et al., 2013) and soil water content (Conant et al.,
82 2004; Davidson et al., 2006; Liu et al., 2009).

83 Given the uncertainties in quantifying the net carbon response of semiarid ecosystems to
84 climate change, a useful approach for addressing this problem is by combining ecosystem level
85 measurements and numerical modeling. Previous efforts have found misrepresentation in the
86 modeling of semiarid ecosystem carbon fluxes (e.g. Huntzinger et al., 2012; Vargas et al., 2013),
87 net carbon balance (Keenan et al., 2012), and its responses to climate change (Friedlingstein et
88 al., 2013). While simulating water, energy and carbon fluxes remains challenging in semiarid
89 ecosystems (Fisher et al., 2014; Li et al., 2004; Xu et al., 2013), there has been much progress on

90 coupled water-vegetation model representations in recent years (Fatichi et al., 2016b). Included
91 in these advances are more accurate representations of ecosystem processes at shorter temporal
92 scales and the simulation of longer-term phenological variations for different plant functional
93 types (e.g. Ivanov et al., 2008a, 2008b). In addition, finer representations of event-scale and
94 seasonal precipitation effects on vegetation dynamics have been achieved, leading to plant
95 carbon assimilation into a number of pools that are essential for capturing vegetation dynamics
96 (e.g. Fatichi et al., 2016b; Ivanov et al., 2008a, 2008b). Given the importance of heterotrophic
97 respiration in semiarid ecosystems (Cable et al., 2008; Verduzco et al., 2015; Yépez et al., 2007),
98 an appropriate representation of this process is necessary for simulating the annual cycle and
99 interannual variability of NEP as well as identifying the impacts of different climate change
100 drivers (e.g. rising CO₂ and changing meteorological conditions).

101 In this contribution, we combine the mechanistic ecohydrological model of Ivanov et al.
102 (2008a) (TIN-based Real-time Integrated Basin Simulator - Vegetation Generation Interactive
103 Evolution, tRIBS-VEGGIE, model) with the soil carbon model (SCM) of Porporato et al. (2003)
104 to describe ecosystem plant and soil processes (e.g. gross primary productivity, autotrophic and
105 heterotrophic respiration) controlling NEP in a subtropical shrubland in northwestern México. In
106 contrast to prior efforts (e.g. terrestrial biosphere models, Huntzinger et al., 2012), the combined
107 tRIBS-VEGGIE and SCM approach tracks energy, water, temperature and substrate limitations
108 on photosynthesis and respiration from multiple carbon pools using process-level prognostic
109 equations that are tailored to seasonally-dry ecosystems. We use a five-year long record of EC
110 flux and meteorological data (Méndez-Barroso et al., 2014; Villarreal et al., 2016) from a
111 subtropical shrubland as well as remote sensing products to calibrate and test the model
112 simulations for its ability to realistically capture water fluxes, vegetation dynamics and the

113 components of net ecosystem productivity ($NEP = GPP - R_{ECO}$). After model confirmation, we
114 conduct a series of climate change experiments using long-term forcing generated by the
115 stochastic downscaling of a set of climate projections from Taylor et al. (2012) that represent
116 near-future (2030-2045) meteorological and atmospheric CO_2 conditions as well as a historical
117 forcing dataset of equivalent length (1990-2005). We selected the near-future period to avoid the
118 potential for dramatic changes in ecosystem composition due to climate change impacts.
119 Combining tRIBS-VEGGIE and SCM within the climate change experiments allowed us to pose
120 the following questions: (1) What are the mechanisms through which soil-plant processes
121 control NEP in seasonally-dry, semiarid ecosystems?, (2) What, if any, will be the impacts of
122 climate change on NEP and its components in the subtropical shrubland?, and (3) What is the net
123 effect of projected changes in meteorological conditions and atmospheric CO_2 on NEP? As a
124 result, this study aims to understand the potential effects of climate change on ecosystem
125 dynamics and carbon cycling in semiarid areas experiencing strong seasonality.

126

127 **2. Materials and methods**

128 **2.1. Site description**

129 The study site is a subtropical shrubland located ~120 km northeast of Hermosillo,
130 Sonora, México (29.74 °N, 110.53 °W) near the rural town of Rayón at an elevation of 632 m.
131 The local climate is semiarid (Köppen classification BSh) with hot summers and cool winters.
132 The long-term (1961-2009) average annual temperature and precipitation (± 1 standard deviation)
133 are 21.4 ± 6.4 °C and 487 ± 181 mm yr⁻¹, as obtained from Comisión Nacional del Agua station
134 00026181 at Rayón, Sonora. Conditions during the study period (2008-2012) were similar to the
135 long-term average, with a mean annual air temperature (TA) of 22.7 ± 0.6 °C and precipitation
136 (P) of 481 ± 92.8 mm yr⁻¹. Precipitation during the NAM season (July-September) is
137 approximately 76% of the annual total at the site (Vivoni et al., 2010a) leading to a peak in
138 vegetation greenness in the month of August (Méndez-Barroso et al., 2009). Site vegetation is
139 composed of drought-deciduous trees and shrubs, including torote papelío (*Jatropha cordata*),
140 tree ocotillo (*Fouquieria macdougalii*), acacia (*Acacia cochliacantha*), palo verde (*Parkinsonia*
141 *praecox*), Mexican mimosa (*Mimosa distachya*) and velvet mesquite (*Prosopis velutina*) as well
142 as organpipe cactus (*Stenocereus thurberi*). Brown (1994) described the vegetation
143 characteristics of subtropical shrublands (or Sinaloan thornscrub) in greater detail. The site
144 topography is relatively flat in proximity to the EC tower (Vivoni et al., 2010b), while the soils
145 are shallow (~1 m) and classified as regosol-yermosol (INEGI, 2010) with sandy loam (0 to 30
146 cm) and sandy clay (30 to 100 cm) texture. Prior studies further describe the site properties used
147 here for the model application, including the soil hydraulic properties, the vegetation albedo, and
148 structural properties (e.g. Méndez-Barroso et al., 2014; Vivoni et al., 2010a, 2010b).

149
150

151 2.2. Site measurements

152 Meteorological flux measurements were performed using the EC technique (Baldocchi,
153 2003, 2008) using a three-dimensional sonic anemometer (CSAT-3, Campbell Sci.) and an open-
154 path infrared gas analyzer (LI-7500, Li-COR Inc.) placed on a 9 m tower over the tree canopy of
155 around 6 m height and oriented with the prevailing southwest wind direction. Vivoni et al.
156 (2010b) describes the EC installation at the site, including the characteristics of the footprint
157 area. Water vapor and CO₂ concentrations and air temperature were measured at high frequency
158 (20 Hz), collected with a CR5000 datalogger (Campbell Sci.) and processed to 30 min averaged
159 quantities to obtain latent (LE) and sensible heat flux (H) and net ecosystem exchange (NEE) of
160 CO₂, as described in the following section. By convention, negative NEE values indicate
161 ecosystem carbon uptake from the atmosphere, which correspond to a positive net ecosystem
162 productivity (i.e. -NEE = NEP). Net radiation (R_{net}) was measured using a CNR Lite2 (Kipp and
163 Zonen) radiometer, and incoming solar radiation with a CMP3 radiometer (Campbell Sci.).

164 For use in the model, incoming solar radiation was partitioned into direct and diffuse
165 components of the visible (VIS, 0.4-0.7 μm) and near infrared (NIR, 0.7-1.3 μm) bands
166 following the procedures of Spitters (1986), while incoming longwave radiation was estimated as
167 a function of air temperature (Duarte et al., 2006). A humidity and air temperature sensor
168 (HMP45D, Vaisala) was used to obtain vapor pressure (VP) and air temperature. Volumetric soil
169 water content (SWC) was obtained as the average of two reflectometer (CS616-L, Campbell
170 Sci.) measurements at a 10 cm depth over the period 2008-2010 and from a soil moisture sensor
171 (ECH2O probe, Decagon Devices) at the same depth and location for portions of 2012. No
172 additional soil moisture sensors at larger soil depths were available. Local precipitation was
173 measured with a tipping-bucket rain gauge (TB4, Hydrological Services). All meteorological

174 measurements were recorded as 30 min averages within the CR5000 datalogger and averaged to
175 hourly inputs for the model applications. Additional information on measurements is presented
176 by Méndez-Barroso et al. (2014), Villarreal et al. (2016) and Vivoni et al. (2010a).

177 Several data gaps occurred during the 2008-2012 period (i.e. 15 to 26% of measurements
178 during all years, except 2008 with 63% missing data since observations started in the summer).
179 We followed the procedure of Robles-Morua et al. (2012) to fill in the necessary meteorological
180 forcing. This process consisted of bias-correcting the surface meteorological data obtained from
181 the North American Land Data Assimilation System (NLDAS) (Mitchell et al., 2004) in the grid
182 pixel (12 km) corresponding to the study site during periods of simultaneous ground data. Linear
183 corrections were applied to hourly variables of atmospheric pressure, incoming solar radiation
184 and vapor pressure, while air temperature was corrected using the adiabatic lapse rate ($6.5\text{ }^{\circ}\text{C}$
185 km^{-1}) to match the site elevation. A logarithmic profile adjustment was used to modify the 10 m
186 NLDAS wind speed to 2 m height assumed for all forcing variables in the ecohydrological model
187 (tRIBS-VEGGIE). The use of bias-corrected NLDAS products to gap-fill the ground-based data
188 was deemed important to create a continuous series of meteorological forcing.

189 In addition, we utilized remotely-sensed data from the Moderate Resolution Imaging
190 Spectroradiometer (MODIS; ORNL DAAC, 2008) to test the model representation of vegetation
191 dynamics, following Méndez-Barroso et al. (2014). Cloud-free composites of the Normalized
192 Difference Vegetation Index (NDVI, 16 day, 250 m, MOD13Q1) and Leaf Area Index (LAI, 8
193 day, 1 km, MOD15A2) were linearly interpolated to a daily product for this purpose. Due to its
194 higher temporal resolution, we report the model evaluation against LAI for assessing vegetation
195 dynamics. Previous research in semiarid areas has been shown to find good agreement between
196 ground-based vegetation conditions and MODIS (i.e. Fensholt et al., 2004; Jenerette et al., 2010),

197 but it should be noted that there are discrepancies between the site conditions and inferred
198 variables of the remote sensing products due to different spatio-temporal resolutions and
199 sometimes due to scattering and absorption by the atmospheric composition (Nagol et al., 2009).

200

201 **2.3. Flux quality control and partitioning**

202 Conventional corrections were applied to EC measurements following Scott et al. (2004),
203 including removal of outliers (gas concentrations greater than ± 4 standard deviations, Massman,
204 2001), a correction for density fluctuations (Webb et al., 1980) and the application of the double
205 rotation method (Wilczak et al., 2001). In addition, friction velocity (u^*) was calculated
206 according to quantitative methods (Scott et al., 2004) and periods of time with a friction velocity
207 less than $u^* = 0.20 \text{ m s}^{-1}$ were filtered (Aubinet et al., 2000; Xu & Baldocchi, 2004) to reduce
208 nighttime flux underestimation (Barr et al., 2013). The u^* threshold was selected such that there
209 is no dependence between nighttime fluxes and friction velocity. Resulting data gaps were filled
210 in following the procedures of the Eddy Covariance Gap-Filling and Flux-Partitioning Tool
211 available at: <http://www.bgc-jena.mpg.de/~MDIwork/eddyproc/index.php>, following Reichstein
212 et al. (2005). The surface energy balance was evaluated at the study site by Villarreal et al.
213 (2016) over 2008-2010 (a closure of 0.89) and Méndez-Barroso et al. (2014) over summers in
214 2006-2009 (a closure of 0.75). The partitioning of NEE into its components GPP and R_{ECO} (i.e.
215 $\text{NEE} = R_{\text{ECO}} - \text{GPP}$) was carried out using the sensitivity of R_{ECO} to air temperature (Flanagan et
216 al., 2002; Reichstein et al., 2005). This NEE partitioning approach has been shown to be
217 consistent with other methods (Babst et al., 2014; Desai et al., 2008).

218

219

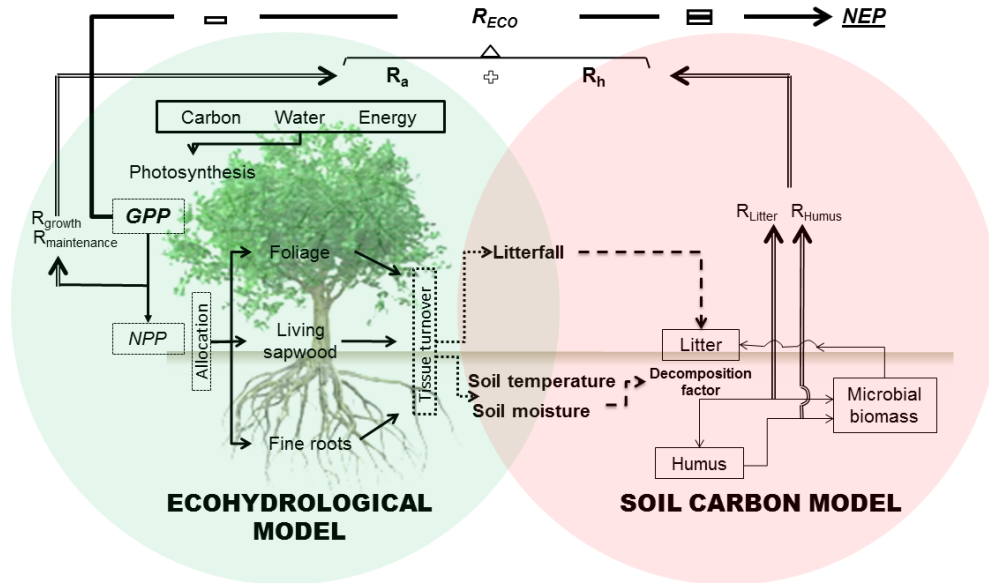
220

221

222

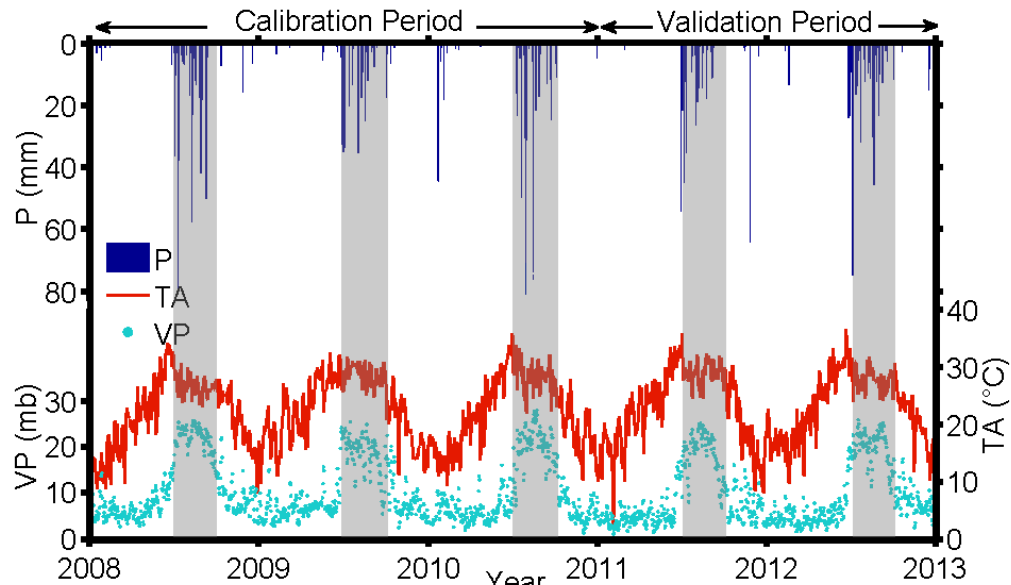
223 2.4. Ecohydrological and soil carbon modeling

224 Water, energy and carbon dynamics at the subtropical shrubland were simulated using a
225 combination of an ecohydrological model (tRIBS-VEGGIE, Ivanov et al., 2008a, 2008b) and a
226 soil carbon model (SCM, Porporato et al., 2003) coupled through the production of litter and the
227 soil moisture and temperature conditions (Fig. 1). Following prior efforts in semiarid regions
228 (Bisht, 2010; Sivandran & Bras, 2012), a drought-deciduous C3 shrub was used as the plant
229 functional type in the one-dimensional simulations using an irregular subsurface mesh (25 layers
230 over 1 m depth). In addition to vertically-resolved soil hydrologic and thermal dynamics, tRIBS-
231 VEGGIE captures a set of biophysical and biochemical plant processes, such as photosynthesis,
232 autotrophic respiration (R_a), carbon allocation to foliage, sapwood and fine roots, tissue turnover
233 and vegetation phenology. This allows the estimation of gross and net ($NPP = GPP - R_a$) primary
234 productivity for the plant functional type. The time-evolving plant conditions are directly
235 affected by and provide an influence on the local energy and water budget in an interactive
236 fashion (Ivanov et al., 2008a, 2008b). Simulated soil water content (SWC), surface energy fluxes
237 (R_{net} , H and LE), total evapotranspiration (ET) and leaf area index (LAI), among others, depend
238 on local meteorological conditions, soil properties and plant functional traits obtained via local
239 measurements or parameterized through a model calibration and validation procedure. Overall,
240 tRIBS-VEGGIE simulates the dynamic feedbacks between vegetation and its surrounding
241 environment at differing time scales, explicitly represented starting at the scale of a few minutes
242 (e.g. resolving canopy leaf temperatures), to hourly resolution (e.g. stomatal dynamics) and up to
243 the daily scale processes (e.g. plant phenology and leaf turnover). Ivanov et al. (2008a, 2008b)
244 provide additional details on the model biophysics and its application in other semiarid settings.



245 **Figure 1.** Conceptual diagram of model-based estimation of ecosystem carbon fluxes
 246 using tRIBS-VEGGIE and SCM. Dotted lines depict ecohydrological model outputs into the soil
 247 carbon model, while double lines specify sources of autotrophic, heterotrophic and ecosystem
 248 respiration ($R_{ECO} = R_a + R_h$). Net ecosystem productivity (NEP) is obtained as $GPP - R_{ECO}$.
 249
 250

251 As depicted in Fig. 1, tRIBS-VEGGIE does not simulate soil heterotrophic respiration
 252 (R_h), limiting its ability to represent net ecosystem productivity ($NEP = GPP - R_a - R_h$). To
 253 address this, we implemented a simplified version of the soil carbon model (SCM) of Porporato
 254 et al. (2003) based on three separate carbon pools (litter, humus and microbial biomass) to track
 255 soil organic matter decomposition and heterotrophic respiration (Bolker et al., 1998; Manzoni et
 256 al., 2004; Parolari & Porporato, 2016). While this approach does not track nitrogen dynamics, we
 257 accounted for C:N effects on decomposition rates through the use of a heuristic factor ϕ
 258 described in Rodríguez-Iturbe & Porporato (2007) and based values either on local data or
 259 magnitudes reported for the region (Martínez-Yrizar et al., 2007; Núñez et al., 2001). Daily
 260 carbon pool dynamics simulated in the SCM were driven by soil water content and temperature
 261 conditions and the leaf litter production derived from tRIBS-VEGGIE. As a result, the coupling
 262 of tRIBS-VEGGIE and SCM allows for the effects of vegetation phenology (i.e. leaf senescence
 263 and fall) to impact R_h and NEP when soil moisture and temperature conditions are favorable.



264 **Figure 2.** Mean daily meteorological conditions during the study period (2008-2012)
 265 consisting of precipitation (P), air temperature (TA) and vapor pressure (VP). Shaded areas
 266 represent NAM period (July-September) of each year.
 267
 268

269 2.5. Model forcing, parameterization and validation

270 Gap-filled meteorological observations over the period 2008-2012 were aggregated to
 271 hourly resolution as forcing for tRIBS-VEGGIE and consisted of atmospheric pressure, vapor
 272 pressure, air temperature, wind speed, incoming solar and longwave radiation and precipitation.
 273 In addition, direct and diffuse radiation components in the visible and near infrared bands and the
 274 average atmospheric CO₂ concentration during 2008-2012 (390 ppm) were input. Fig. 2 presents
 275 an example of the meteorological forcing, illustrating the strong seasonality in precipitation and
 276 its corresponding effects on air temperature and vapor pressure during the NAM.

277 The study period was divided into two subsets for model calibration (2008-2010, 1096
 278 days) and validation (2011-2012, 731 days) based upon matching the subset length when
 279 excluding gap-filled periods. While conditions varied to some extent among the subsets, no
 280 trends were noted that would impact model calibration and validation. A similar setup was
 281 carried out for the SCM by using leaf litterfall, soil moisture and soil temperature conditions

282 obtained from tRIBS-VEGGIE as inputs (Fig. 1). Following Vivoni et al. (2005), the sequence of
283 tRIBS-VEGGIE and SCM simulations were conducted in a periodic fashion by repeating the
284 same 5-yr meteorological forcing 6 times (i.e. total simulation length of 30 years) and retaining
285 the two subsets in the last 5-yr period for model calibration and validation purposes. This
286 initialization approach stabilized soil water content, soil temperature and carbon storage amounts
287 in the vegetation (foliage, sapwood and fine roots) and soil (litter, microbial biomass and humus)
288 pools, thus reducing transient errors in the assignment of the initial conditions.

289 Initial model parameterization was conducted for tRIBS-VEGGIE and SCM based upon
290 prior efforts with each model (e.g. Bisht, 2010; Ivanov et al., 2008a; Parolari & Porporato, 2016;
291 Porporato et al., 2003; Sivandran & Bras, 2012), including applications for the subtropical
292 shrubland (Méndez-Barroso et al., 2014; Vivoni et al., 2010a). For instance, Table 1 presents the
293 soil hydraulic and thermal properties used in tRIBS-VEGGIE for the sandy loam soils at the site
294 whose initial values were obtained through manual calibration conducted by Méndez-Barroso et
295 al. (2014). As in that work, we simplified the modeling of site conditions by treating the soil
296 profile as a uniform sandy loam. In contrast to Méndez-Barroso et al. (2014), however, we
297 applied the one-dimensional Richards equation using a finite element, backward Euler time
298 stepping numerical approximation for infiltration into the unsaturated soil profile (irregular mesh
299 with 25 layers over 1 m depth), as detailed in Ivanov et al. (2008a). Accordingly, modifications
300 to the soil parameters within feasible ranges based on pedotransfer functions from Rawls et al.
301 (1982) were required to match a larger set of observations (SWC, R_{net} , H, LE and LAI) over a
302 longer period (i.e. three continuous years in the calibration period).

303 An invariant rooting profile extending to 1 m depth and a vegetation fraction ($v_f = 0.6$)
304 were estimated for the study site following Jackson et al. (1996) and Méndez-Barroso et al.

<i>Soil Type</i>	Sandy Loam
K_s	55
θ_s	0.45
θ_r	0.02
λ_o	0.47
ψ_b	-90
$k_{s,dry}$	0.214
$k_{s,sat}$	2.64
C_s	1610586

Table 1. Soil Parameters. K_s (mm hr⁻¹), surface hydraulic conductivity; θ_s (-), saturated moisture content; θ_r (-), residual moisture content; λ_o (-), pore size distribution index; ψ_b (mm), air entry bubbling pressure; $k_{s,dry}$ and $k_{s,sat}$ (J m⁻¹ s⁻¹ K⁻¹), heat conductivity for dry and saturated soils; C_s (J m⁻³ K⁻¹), heat capacity of dry soils.

(2014). In addition, tRIBS-VEGGIE required a larger set of model parameters to describe biochemical, biophysical, interception, phenological, carbon allocation and water uptake processes (Ivanov et al., 2008a). Table 2 lists the final parameter values for vegetation processes and indicates their sources as either from literature (L), observation (O) or calibration (C).

<i>Parameter</i>	<i>Value</i>	<i>Source</i>
Biochemical Processes		
V_{max25}	50	C
K	0.2	C
M	9	L
B	10000	L
$\epsilon_{3,4}$	0.08	L
r_{sapw}	9.61×10^{-10}	L
r_{root}	1.09×10^{-8}	L
w_{grw}	0.25	L
d_{leaf}	1	L
d_{sapw}	0.04	L
d_{root}	0.33	L
Biophysical and Interception Processes		
χ_L	0.01	L
α_{leaf} (VIS, NIR)	0.1, 0.45	L
α_{stem} (VIS, NIR)	0.16, 0.39	L
τ_{leaf} (VIS, NIR)	0.05, 0.25	L
τ_{stem} (VIS, NIR)	0.001, 0.001	L
K_c	0.18	L
g_c	3.9	L

S_{la}	0.011	O
Phenology, Allocation and Uptake Processes		
γW_{max}	10	C
b_w	2.5	C
γC_{max}	7	C
b_c	1	C
T_{cold}	15	C
e_{leaf}	0.25	L
e_{sapw}	0.1	L
e_{root}	0.65	L
ω	0.8	L
ϵ_s	2	L
ξ	1.6	L
T_{soil}	20	C
D_{LH}	10	L
$D_{Tmin,Fav}$	6	C
$f_{c,init}$	0.025	L
L_{init}	0.22	L
ψ^*	-0.1	C
ψ_w	-5	C

314 **Table 2. Vegetation Parameters.** V_{max25} ($\mu\text{mol CO}_2 \text{ m}^{-2} \text{ leaf s}^{-1}$) is the maximum
315 catalytic capacity of Rubisco at 25°C; K (-) is the time-mean PAR extinction coefficient
316 parameterizing the decay of nitrogen content in the canopy; m (-) is an empirical slope
317 parameter; b ($\text{mmol m}^{-2} \text{ s}^{-1}$) is the minimum stomatal conductance; $\epsilon_{3,4}$ ($\mu\text{mol CO}_2 \mu\text{mol}^{-1}$
318 photons) is the intrinsic quantum efficiency for CO_2 uptake; r_{sapw} and r_{root} ($\text{g C g C}^{-1} \text{ s}^{-1}$) are the
319 sapwood and fine root respiration coefficients at 10°C; w_{grw} (-) is the fraction of canopy
320 assimilation less maintenance respiration used for tissue growth; d_{leaf} , d_{sapw} and d_{root} (yr^{-1}) are the
321 turnover rates for leaf, sapwood and roots; χL (-) is the departure of leaf angles from a random
322 distribution; α_{leaf} and α_{stem} (-) are the leaf and stem reflectances in the VIS and NIR bands; τ_{leaf}
323 and τ_{stem} (-) are leaf and stem transmittances in the VIS and NIR bands; K_c (mm hr^{-1}) is the
324 canopy drainage coefficient, g_c (mm^{-1}) is the exponential decay parameter of canopy water
325 drainage; S_{la} ($\text{m}^2 \text{ leaf area kg C}^{-1}$) is the specific leaf area; γW_{max} and γC_{max} (day^{-1}) are maximum
326 drought and cold-induced foliage loss rates; b_w and b_c (-) are the shape parameters reflecting the
327 sensitivity of canopy to drought and cold; T_{cold} ($^{\circ}\text{C}$) is the temperature threshold below which
328 cold-induced leaf loss begins; e_{leaf} , e_{sapw} and e_{root} (-) are the base allocation fractions for leaf,
329 sapwood and roots; ω (-) is the sensitivity parameter of allocation fractions to changes in light
330 and water availability; ϵ_s and ξ (-) are parameters controlling the relation between carbon content
331 in the above and below ground biomass; T_{soil} ($^{\circ}\text{C}$) and D_{LH} (hr) are the mean daily soil
332 temperature and day length to be exceeded for the growing season start; $D_{Tmin,Fav}$ (day) is the
333 minimum duration for which the conditions of transition from/to the dormant season have to be
334 continuously met; $f_{c,init}$ and L_{init} (-) are the fraction of the structural biomass and leaf area index
335 used to initiate leaf onset; ψ^* and ψ_w (MPa) are the soil matric potentials at which the stomatal
336 closure and plant wilting begins.
337

<i>Parameter</i>	<i>Value</i>	<i>Source</i>
C_l	89	L
C_h	895	L
C_b	25	L
C/N_{litter}	23	O
C/N_{humus}	22	L
C/N_{biomass}	8	L
r_h	0.003	L/C
r_r	0.65	L
k_b	0.0000988	C
k_h	2.1×10^{-7}	C
k_l	0.00107	C

Table 3. Soil Decomposition Parameters. C_l , C_h and C_b (g C m^{-2}) are initial carbon concentrations in the litter, humus and biomass pools; C/N_{litter} , C/N_{humus} and C/N_{biomass} (-) are carbon-nitrogen ratios of litter, humus and biomass; r_h and r_r (-) are fractions of organic matter undergoing humification and of decomposed organic carbon that is respired; k_l , k_h and k_b (hr^{-1}) are first-order kinetic constants of litter, humus and biomass.

Manual calibration of vegetation parameters focused on capturing the LAI dynamics during 2008-2010 as observed from MODIS during the NAM growing season. A one-at-a-time sensitivity analysis was conducted to identify the importance of each parameter on the simulation of LAI and limit the sampling necessary for model calibration. Similarly, a manual calibration approach was used for the SCM parameters (Table 3). We used observations of SCM model parameters or initial conditions when available from the site or nearby areas (e.g. Búrquez et al., 1999; Martínez-Yrizar et al., 1999; 2007; Núñez et al., 2001; Pavón et al., 2005). Though manual calibration was conducted, the combined models are amenable to automated estimation methods (e.g. Duan et al., 1993) due to the low computational demands for single site applications. The combination of tRIBS-VEGGIE and SCM allowed for simulation of $R_{\text{ECO}} = R_a + R_h$ that was compared to R_{ECO} observations derived from the EC method during calibration and subsequently permitted a comparison of NEP between observations and simulations. We validated the model performance using a comparison between simulated and observed values of the aforementioned variables during the 2011-2012 period, which was not used in the model calibration effort.

358 **2.6. Climate change and CO₂ fertilization experiments**

359 We obtained air temperature (monthly) and precipitation (3-hr) projections from the
360 Coupled Model Intercomparison Project version 5 (CMIP5) (Taylor et al., 2012) for three
361 General Circulation Models (GCMs) selected for their ability to represent the NAM system (Geil
362 et al., 2013): CNRM-CM5, HadGEM2-ES and MIROC5. Single realizations from each model
363 were selected for a near-future period (2030-2045) under the RCP8.5 emissions case (IPCC,
364 2013), selected to match the 15-yr length of a historical forcing period (1990-2005) obtained
365 from NLDAS (labeled as 'HIST'). Given the hourly meteorological forcing requirements of
366 tRIBS-VEGGIE, we implemented the stochastic downscaling method of Fatichi et al. (2013) to
367 apply a set of factors of change derived from the individual GCMs and their averaged conditions
368 (referred to hereafter as 'AVE') to the statistical properties obtained from the historical forcing.
369 For each scenario, sets of change factors were calculated separately for the statistical properties
370 of precipitation (e.g. mean, variance, skewness and frequency of no-precipitation at different
371 aggregation periods (1, 6, 24, 72 hours) and mean monthly air temperature). Since GCM
372 realizations were obtained at a 3-hr interval, we followed Fatichi et al. (2011) to extend the
373 statistical properties to a finer hourly resolution for the full set of meteorological forcings
374 (atmospheric pressure, wind speed, incoming solar and longwave radiation, air temperature,
375 vapor pressure and precipitation). Since our study periods were relatively short (15-yr), we
376 utilized the derived statistical metrics from the method of Fatichi et al. (2013) to generate
377 synthetic (100-yr long) hourly forcings for each scenario (HIST, CNRM-CM5, HadGEM2-ES,
378 MIROC5 and AVE). These should be considered as representative realizations of the climate
379 system under stationary historical and near-future conditions, as simulated by these GCMs,
380 allowing statistical sampling to be conducted. Two sets of simulations were performed for each

381 scenario to differentiate the effects of CO₂ fertilization from meteorological changes: (1) No
382 fertilization cases used the average of 365 ppm calculated from historical CO₂ concentrations
383 from 1990-2005 and (2) CO₂ fertilization cases with a constant concentration of 482 ppm,
384 obtained from RCP8.5 from 2030-2045 period (about a 32% increase in CO₂ above historical).
385 Since we are simulating synthetic 100-yr long scenarios, it was necessary to use a constant CO₂
386 concentration that best represent the conditions for each period (i.e., 1990-2005 and 2030-2045).

387

388 **3. Results and discussion**

389 **3.1. Evaluation of simulated water, energy and carbon dynamics**

390 Simulated water, energy and carbon states and fluxes in the subtropical shrubland were
391 compared to available observations over the calibration, validation and full study periods using
392 three metrics: correlation coefficient (CC), bias (B) and mean absolute error (MAE) (Vivoni et
393 al., 2006). Table 4 shows the metrics obtained for daily-averaged and hourly values, with a CC
394 near one, a bias close to unity and a low MAE indicating a good match between the observed and
395 simulated variables at both time scales and for all variables. For instance, the simulated surface
396 energy fluxes (R_{net} , H and LE) exhibit a good correspondence to observations, with high CC (>
397 0.77), B near unity (within ± 0.16) and an MAE less than 33 W m^{-2} for hourly and daily values.
398 Fig. 3 illustrates the model performance with respect to the surface energy fluxes by comparing
399 seasonal cycles of R_{net} , H and LE over the full study period. Note the dramatic change in the
400 partitioning of R_{net} into H and LE upon the onset of the NAM in July, with the arrival of summer
401 storms increasing LE (or ET) substantially. Overall, the ecohydrological model adequately
402 captures monthly variations in the surface energy fluxes, though a consistent underestimation of
403 R_{net} of 14.4 W m^{-2} is noted from December through June due to the lack of simulated vegetation
404 (i.e. a decrease in LAI and a corresponding increase in albedo) affecting the absorption of solar

Variable	Calibration period 2008-2010			Validation period 2011-2012			Full period 2008-2012			
	CC	B	MAE	CC	B	MAE	CC	B	MAE	
Daily Values	SWC ($\text{m}^3 \text{m}^{-3}$)	0.86	0.91	0.03	0.93	0.65	0.01	0.86	0.83	0.02
	ET (mm)	0.91	0.81	0.01	0.94	0.89	0.02	0.92	0.84	0.01
	LAI (-)	0.88	1.06	0.39	0.91	1.00	0.36	0.89	1.04	0.38
	R_{net} (W m^{-2})	0.85	0.91	19.46	0.97	0.87	15.05	0.91	0.90	17.70
	LE (W m^{-2})	0.91	0.81	9.22	0.94	0.89	11.2	0.92	0.84	10.01
	H (W m^{-2})	0.76	1.16	16.88	0.82	0.91	18.16	0.77	1.04	17.39
	GPP (g C m^{-2})	0.85	0.92	0.04	0.83	1.16	0.04	0.85	1.05	0.04
	R_{ECO} (g C m^{-2})	0.90	1.09	0.02	0.88	1.16	0.02	0.90	1.12	0.02
	NEP (g C m^{-2})	0.58	0.99	0.03	0.67	0.95	0.03	0.60	0.78	0.03
Hourly Values	SWC ($\text{m}^3 \text{m}^{-3}$)	0.80	0.91	0.03	0.90	0.65	0.01	0.81	0.83	0.02
	ET (mm)	0.86	0.81	0.02	0.79	0.88	0.03	0.83	0.84	0.03
	R_{net} (W m^{-2})	0.96	0.91	28.23	0.97	0.87	31.33	0.96	0.90	29.47
	LE (W m^{-2})	0.86	0.81	15.98	0.79	0.88	22.2	0.83	0.84	18.48
	H (W m^{-2})	0.90	1.16	24.65	0.91	0.91	45.33	0.90	1.04	32.92
	GPP (g C m^{-2})	0.70	1.08	0.07	0.75	1.29	0.05	0.72	1.15	0.06
	R_{ECO} (g C m^{-2})	0.73	1.09	0.04	0.69	1.16	0.04	0.71	1.12	0.04
	NEP (g C m^{-2})	0.58	0.97	0.07	0.63	0.94	0.06	0.60	0.78	0.06

Table 4. Model Performance Metrics for Daily and Hourly Values. Correlation coefficient (CC), Bias (B) and Mean Absolute Error (MAE) are calculated for soil water content (SWC), evapotranspiration (ET), leaf area index (LAI), net radiation (R_{net}), sensible heat flux (H), gross primary productivity (GPP), ecosystem respiration (R_{ECO}) and net ecosystem productivity (NEP) during calibration, validation and full periods.

radiation, comparable to prior studies (Ivanov et al., 2008a). In addition, tRIBS-VEGGIE simulation tends to slightly overestimate sensible heat flux from May to August by an average of $12.7 \pm 3.8 \text{ W m}^{-2}$, despite adequately capturing the latent heat flux, though the difference is within the monthly standard deviation (error bars) obtained across all years. Overall, monthly, daily and hourly comparisons demonstrate the robust capability of tRIBS-VEGGIE to capture surface energy fluxes, themselves tied to soil water content and vegetation conditions.

Fig. 4 presents observed and simulated SWC in the top 10 cm, LAI dynamics and litterfall variations during the calibration and validation periods, and simulated soil temperature (T_{soil}) derived from tRIBS-VEGGIE that are critical inputs to the SCM. Note how the summer rainy

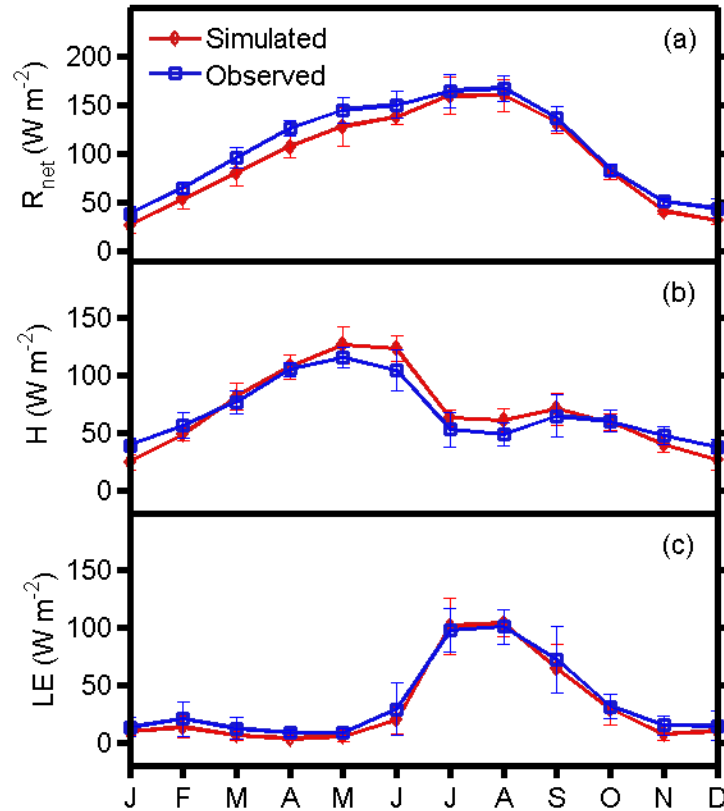
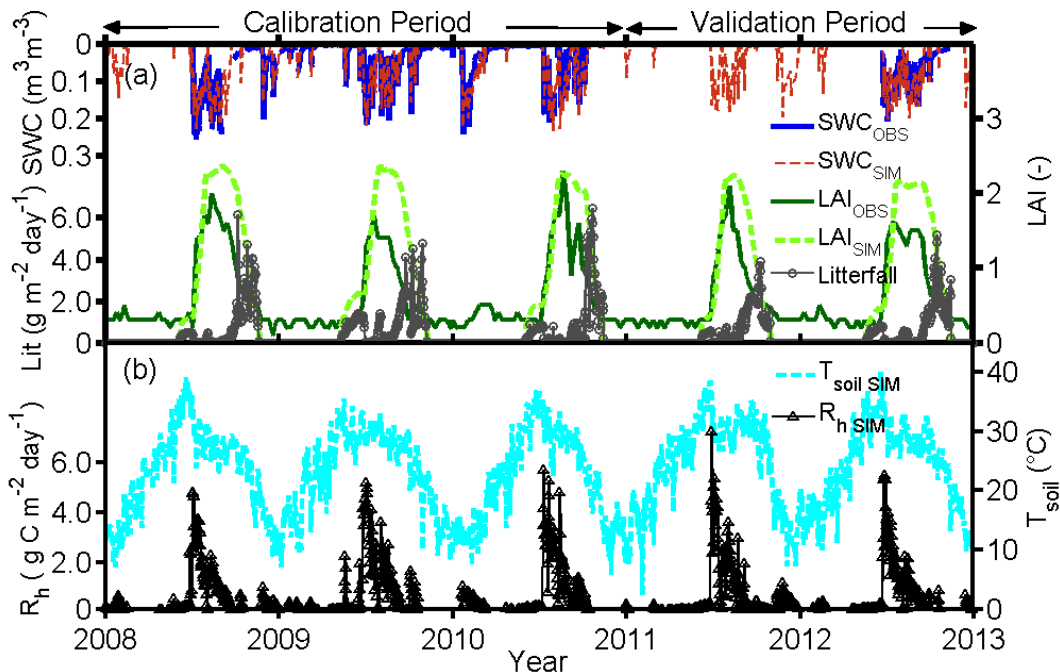


Figure 3. Seasonal cycle of observed versus simulated surface energy fluxes over the study period (2008-2012): (a) net radiation (R_{net}), (b) sensible heat flux (H) and (c) latent heat flux (LE). Symbols are monthly averages and ± 1 standard deviation as error bars.

season during the NAM leads to increases in SWC that were accurately captured by the model, as described in Table 4, with the tRIBS-VEGGIE model serving as an effective tool to interpolate within periods of observed data gaps. Simulated LAI captured well the primary summer growing season ($CC \geq 0.88$, B within 0.06 of unity, $MAE \leq 0.39$) and the differences between years. However, the model did not capture the observed (MODIS-based) LAI variations during the winter period, as noted by Bisht (2010). This is likely due to representing only the drought-deciduous component of the ecosystem (C3 shrubland) and possible issues related to the scale discrepancy between MODIS-based LAI estimates and the model application. Although this might lead to small errors in the estimation of annual biomass, the particularly strong summer season minimizes the role played by the winter in terms of physiological activity, as has

435 been noted with carbon fluxes in the NAM region (e.g. Huxman et al., 2004b; Pérez-Ruiz et al.,
436 2010; Scott et al., 2004; Verduzco et al., 2015). Correspondingly, model estimates of GPP were
437 adequate at the hourly resolution as compared to derived values from the EC measurements and
438 improved substantially at the daily resolution (Table 4), though we noted that overestimation
439 during the NAM was typical ($B = 1.23$). Although LAI and the foliage carbon pool appears to
440 have low interannual variations, the simulations of GPP that account for all carbon pools (root,
441 stem and foliage) correspond well with observations and demonstrate higher values during wetter
442 years, as expected. The few available data on T_{soil} limited the possible tests of the model, though
443 for 2011, tRIBS-VEGGIE matched the observations very well ($CC = 0.97$, $B = 0.99$ and $MAE =$
444 $1.9\text{ }^{\circ}\text{C}$ for hourly values).

445 After the NAM ends, soil moisture and temperature conditions become less favorable for
446 the drought-deciduous plants and the subtropical shrubland transitioned into dormancy (low LAI
447 by November) after a complete foliage turnover (Fig. 4). Litterfall was simulated by tRIBS-
448 VEGGIE to account for about 30% of the GPP each year, with values ranging from 120 to 180 g
449 $\text{C m}^{-2} \text{ yr}^{-1}$, consistent with studies in the Sonoran Desert ($\sim 157\text{ g C m}^{-2} \text{ yr}^{-1}$) (Martínez-Yrizar et
450 al., 1999). Along with the simulated SWC and T_{soil} conditions, litterfall determined inputs to the
451 SCM from which heterotrophic respiration (R_h) fluxes were simulated (Fig. 4b). Simulated
452 carbon amounts in the litter and microbial biomass pools ranged from 20 to 200 g C m^{-2} and
453 from 70 to 130 g C m^{-2} , respectively, whereas the carbon amount in the humus pool remained
454 relatively stable at 895-900 g C m^{-2} during the study period, similar to measured values in
455 semiarid shrublands (e.g. Bolton et al., 1993; Cardoso et al., 2015; Cheng et al., 2015; Goberna
456 et al., 2007). As expected, low amounts of R_h occur during the winter and spring and increase
457 substantially after the first rainfall event during the NAM due to the available SWC and labile



458 **Figure 4.** (a) Comparison of daily observed (OBS) and simulated (SIM) soil water
 459 content (SWC) and leaf area index (LAI). Simulated Litterfall (Lit) in (a), soil temperature (T_{soil})
 460 and heterotrophic respiration (R_h) in (b) from tRIBS-VEGGIE (Litterfall, T_{soil}) and SCM (R_h).
 461
 462

463 substrate, consistent with Verduzco et al. (2015) and Zhang et al. (2014). Simulated litter
 464 decomposition decreased as the labile substrate amounts were depleted which leads to a
 465 reduction in the microbial biomass pool, similar to observations made in long-term incubation
 466 studies (Follett et al., 2007; Steinweg et al., 2008). As a result, the heterotrophic respiration was
 467 highly sensitive to the arrival of early storms during the NAM warm season, through its impact
 468 on SWC, and to the amount of labile substrate from the previous summer season, via the litterfall
 469 occurring at the end of the prior NAM.

470 By capturing R_h in the SCM, the simulated ecosystem respiration ($R_{\text{ECO}} = R_a + R_h$) was
 471 compared to EC measurements in Fig. 5. Table 4 indicates a good correspondence between the
 472 observed and simulated R_{ECO} (CC > 0.73, B within 0.09 of unity, MAE < 0.04 g C m⁻²) at hourly
 473 and daily resolution. However, we noted discrepancies in the R_{ECO} for summers with high LAI,
 474 suggesting that autotrophic respiration (R_a) for plant growth and maintenance was overestimated
 475 to some extent. In addition, simulated R_{ECO} appeared flashier than the observations at the start of

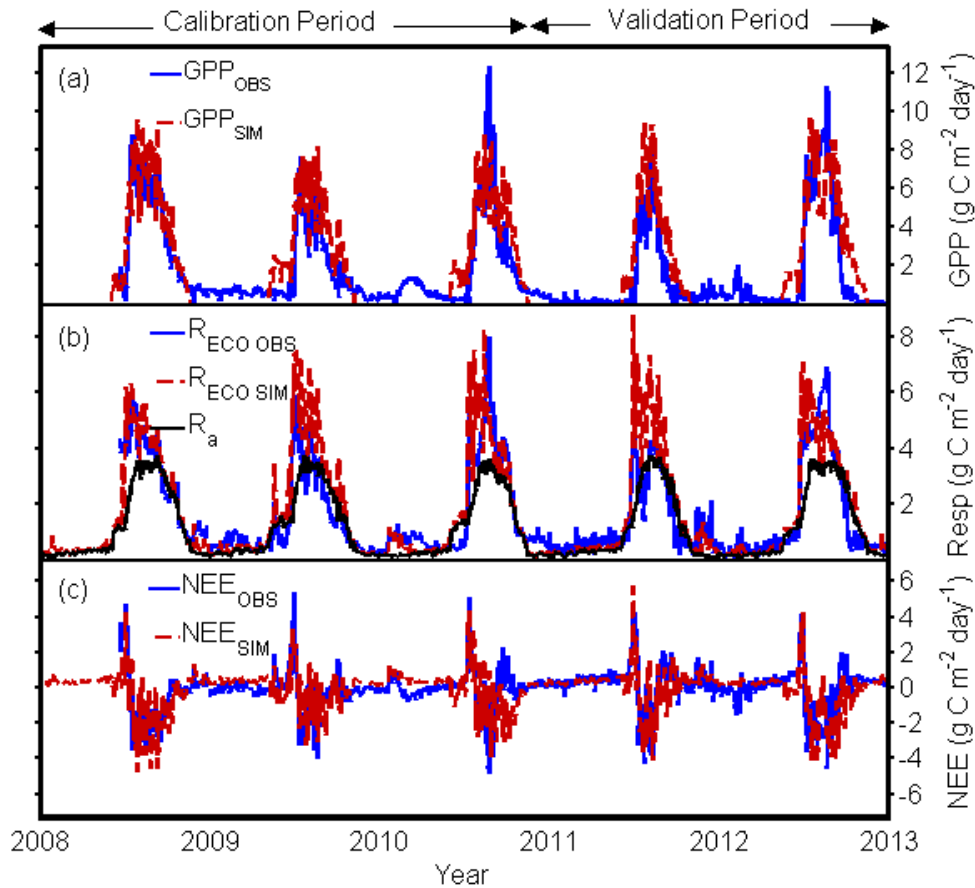


Figure 5. Comparison of observed (OBS) versus simulated (SIM) of (a) gross primary productivity, (b) ecosystem respiration (R_{ECO}) along with simulated autotrophic respiration (R_a) and, (c) net ecosystem exchange. Simulated R_{ECO} was obtained by combining R_a from the ecohydrological model tRIBS-VEGGIE and R_h from the SCM.

the summer season (Fig. 5b) due to rapid changes in R_h when both labile substrate and water were available and soil temperatures are high. As expected, the contribution of R_h to R_{ECO} decreased while the contribution of R_a increased during the temporal progression of the NAM season, reflecting the reduced role of microbial decomposition and the increased role of plant respiration during the growing period (e.g. Carbone et al., 2016).

Fig. 5 and Table 4 also compare observed and simulated GPP, NEE and NEP, respectively, indicating a reasonable match at hourly and daily scales. Note that the positive NEE (carbon loss) occurring early in the summer would not have been possible to represent without simulating R_h in the SCM, consistent with the metabolic activity of microbial communities when

491 high quality litter inputs were available (Carbone et al., 2011; McCulley et al., 2004; Sponseller,
492 2007; Thiessen et al., 2013; Unger et al., 2010). Furthermore, the negative NEE (carbon uptake)
493 during the growing season and the stable values of NEE near zero during the dormant period
494 were accurately captured by the models. Some issues are noted in 2010 which has an observed
495 positive NEE in the late summer season that is not reproduced by the models. Nevertheless,
496 similar patterns of annual NEP were found in the simulations and observations. During the study
497 period, the subtropical shrubland acted as a net sink of carbon during most years (annual NEP
498 from 33 to 105 g C m⁻²), with the exception of 2011, in which both the simulations and
499 observations indicated a net source of carbon (NEP of -53.1 and -98.3 g C m⁻²).

500

501 **3.2. Meteorological changes in historical and climate change experiments**

502 Fig. 6 presents the outcomes of the stochastic downscaling procedure applied to historical
503 (1990-2005, NLDAS) and near-future (2030-2045, CNRM-CM5, HadGEM2-ES, MIROC5 and
504 AVE) periods in terms of the seasonal (monthly) cycle of air temperature and precipitation (a, b)
505 and the probability density functions (PDFs) of summertime TA and P (c, d). These metrics were
506 selected to show the range of meteorological changes in the experiments and summarize the
507 model forcing tailored to the study site (i.e. a full set of hourly variables of 100-yr duration for
508 each scenario). Due to the model performance and the nature of the seasonal dynamics, a focus is
509 placed on the summer season (MJJAS) in the analyses, including a distinction between pre-
510 monsoon (MJ) and monsoon (JAS) periods. As expected from the RCP8.5 emissions case, a
511 strong warming signal is present in the near-future, with increases in mean annual temperature
512 ranging from +1.1 to +2.3 °C with respect to the HIST scenario. HadGEM2-ES exhibited the
513 largest increase in mean summer TA (+2.6 °C), whereas CNRM-CM5 had the lowest increase
514 (+1.0 °C) relative to HIST. When averaged over the three models, the AVE scenario indicates a

515 warming of +1.7 °C in mean summer TA and a shift from a range of 24.4 to 33.6 °C in HIST (± 1
516 standard deviation envelop) to 26.1 to 35.3 °C in AVE (Fig. 6a). These effects are illustrated
517 nicely through the PDFs of summer (MJJAS) average TA, obtained from hourly values over the
518 100-yr sample size (Fig. 6c). Note the increase in summer TA relative to HIST in the order:
519 CNRM-CM5, MIROC5 and HadGEM2-ES. These estimates are consistent with projections for
520 the North American monsoon (Cook & Seager, 2013; Lee & Wang, 2014; Maloney et al., 2014;
521 Pachauri et al., 2014) suggesting a warming signal of +1.4 and 2.7°C between 2035 and 2065.

522 A comparison of the seasonal cycle of precipitation from the scenarios (Fig. 6b) indicates
523 that the use of factors of change in the stochastic downscaling method preserves rainfall
524 seasonality as compared to the historical period with 60 to 80% of the annual precipitation
525 occurring during summer (MJJAS), while leading to the differences in mean summer
526 precipitation amounts (Fig. 6d). Among the GCMs, HadGEM2-ES had lowest mean summer
527 precipitation in the near-future period (327 mm or -21 mm with respect to HIST), whereas
528 MIROC5 exhibited the highest mean summer P (422 mm or +74 mm relative to HIST). When
529 averaged over the three models, the AVE scenario had a nearly identical mean monthly variation
530 of P as HIST (Fig. 6b), with a slightly expanded range of variability in August and October, and
531 a similar distribution of summer total P (Fig. 6d). These comparisons are important since relative
532 precipitation differences among GCMs (i.e. two GCMs have lower P and one has a higher P as
533 compared to HIST) were quite larger than their temperature variations (i.e. all GCMs show rising
534 TA). Precipitation variations in the scenarios might differ from other analysis of the CMIP5
535 models (Cook & Seager, 2013) or other downscaling approaches applied to the NAM region
536 (Castro et al., 2012; Cerezo-Mota et al., 2011) since the historical seasonality at a monthly

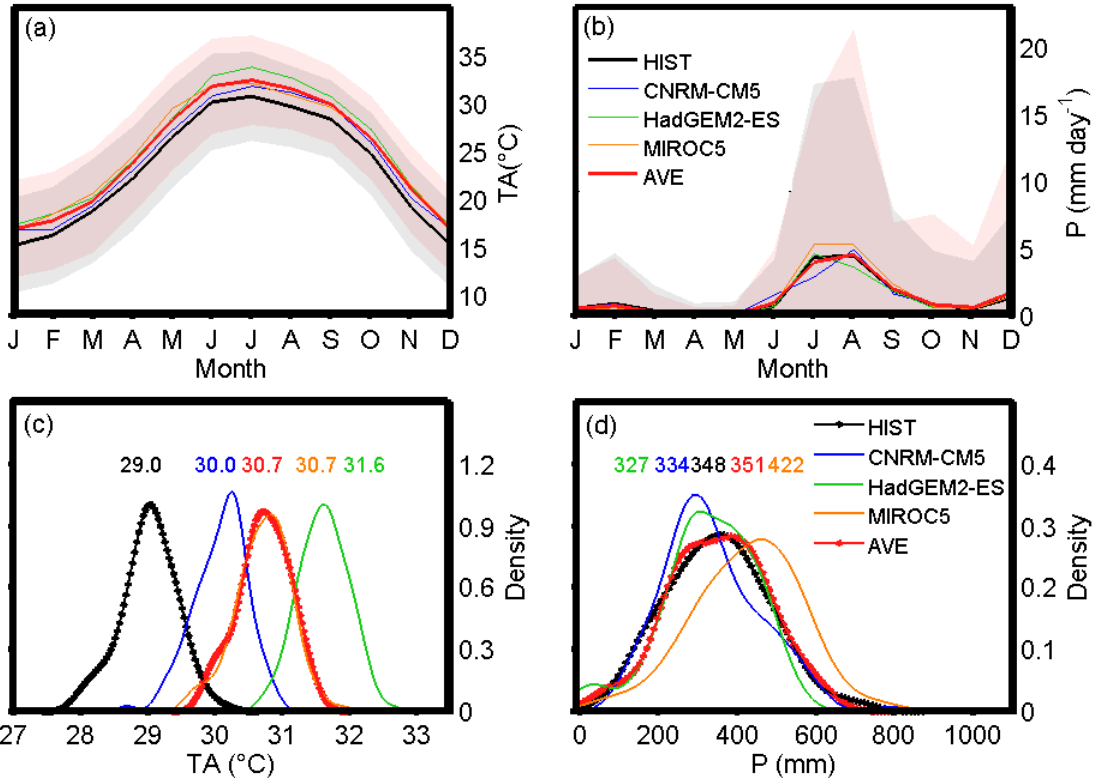
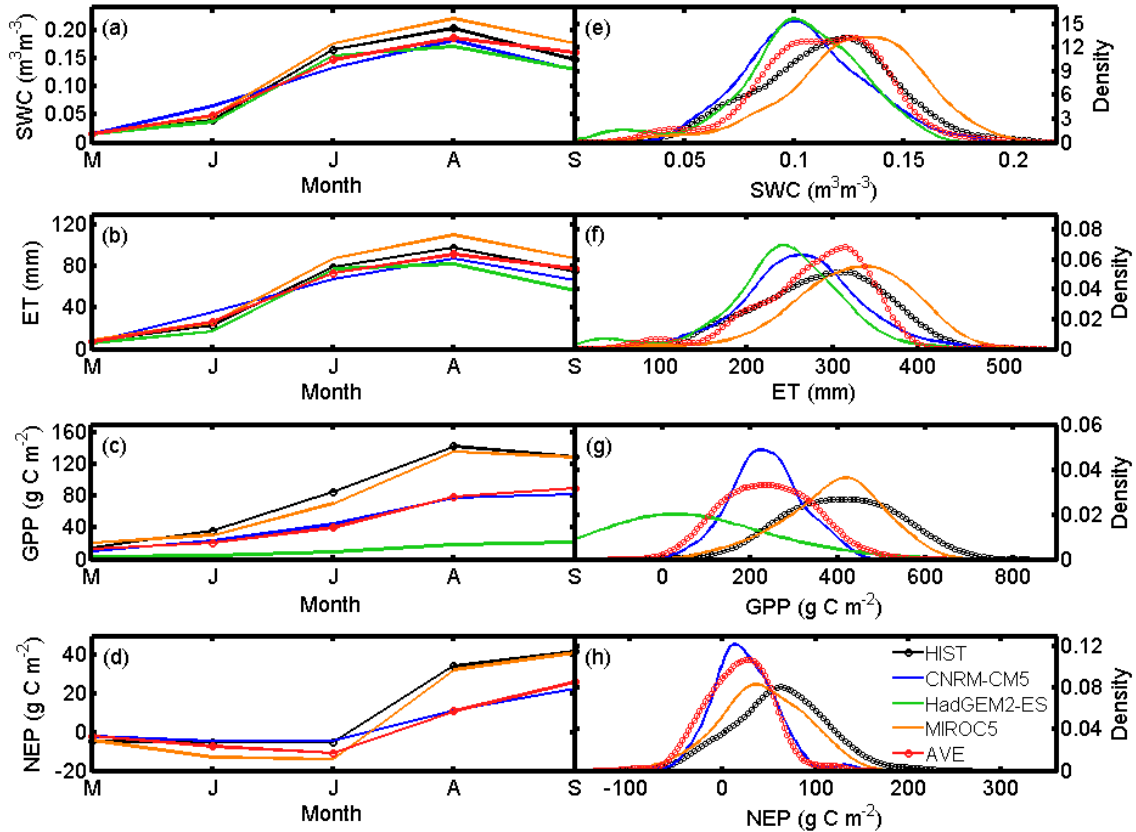


Figure 6. Comparison of meteorological conditions for historical (1990-2005) and climate change experiments (2030-2045) at the study site using representative realizations for HIST, CNRM-CM5, HadGEM2-ES, MIROC5 and AVE. (a, b) Monthly averages of daily air temperature (TA) and precipitation (P) with ± 1 standard deviation shown as a shaded envelope for HIST (gray) and AVE (pink). (c, d) Probability density functions (PDFs) of summer (MJJAS) average TA and total P. Numbers indicate mean values for each case.

resolution was explicitly preserved, rather than allowed to evolve dynamically in the stochastic downscaling approach applied (Fatichi et al., 2013). Nevertheless, the considered scenarios captured a range of plausible near-future precipitation conditions, including increasing, decreasing or no net change in summer amounts, under a warming trend that are considered realistic for the purposes of identifying climate change impacts.

3.3. Meteorological change effects on simulated water, energy and carbon dynamics

Responses to meteorological variations imposed by the climate change experiments were assessed first in the absence of increases in atmospheric CO₂ (365 ppm during 1990-2005). Fig.



554

555

556

557

558

559

560

561

562

563

564

565

566

567

568

569

Figure 7. Comparison of water, energy and carbon dynamics for historical (1990-2005) and climate change experiments (2030-2045) using representative realizations for HIST, CNRM-CM5, HadGEM2-ES, MIROC5 and AVE. Monthly mean values and seasonal probability density functions of (a, e) soil water content (SWC), (b, f) evapotranspiration (ET), (c, g) gross primary productivity (GPP) and (d, h) net ecosystem productivity (NEP) during summer (MJJAS).

7 shows the results of the various scenarios (HIST, CNRM-CM5, HadGEM2-ES, MIROC5 and AVE) in terms of the monthly-averaged SWC, ET, GPP and NEP (left panels) during the summer period (MJJAS) as well as the probability density functions of summer season values (right panels), selected to illustrate the rich set of ecohydrological outcomes. The monthly values are obtained as averages over the 100-yr periods, while the probability density functions show the full range of total summer season outcomes from each scenario and thus indicate interannual variability represented for historical and near-future conditions. The imposed air temperature and precipitation changes resulted in substantial summertime variations in the water, energy and carbon dynamics among the climate change experiments. For instance, scenarios with summer

570 precipitation lower than HIST (HadGEM2-ES and CNRM-CM5, Fig. 6d) exhibited decreases in
571 SWC (Fig. 7a,e) and ET (Fig. 7b,f), whereas scenarios with summer P at or above HIST (AVE
572 and MIROC5) showed SWC and ET that were similar to or higher than HIST.

573 The strong correspondence between summer ET and SWC across simulations ($R^2 > 0.88$,
574 $p < 0.05$) is typical of seasonally-dry ecosystems (e.g. Scott et al., 2010; Vivoni et al., 2008).
575 Nevertheless, air temperature differences among the climate change experiments also influenced
576 ET through the sensitivity of plant physiological activity to warming. Specifically, stomatal
577 conductance (g_s) in the simulations was reduced with rising TA for a constant CO_2 value due to
578 increasing vapor pressure deficit and reductions on soil water content (Verduzco, 2016). As an
579 example, the HadGEM2-ES scenario with the highest TA (Fig. 6c) exhibited increased
580 evaporative demand, which causes complete vegetation failure leading to a reduction in ET due
581 to elimination of the transpiration component. This is consistent with field studies in semiarid
582 ecosystems reporting decreased stomatal conductance and carbon assimilation under warming-
583 induced stress (Hamerlynck & Knapp, 1996; Hamerlynck et al., 2000; Ogle & Reynolds, 2002;
584 Serrat-Capdevila et al., 2011).

585 Interestingly, differences among the climate change experiments were more pronounced
586 when comparing carbon dynamics through the monthly evolution and summer total GPP (Fig.
587 7c,g) and NEP (Fig. 7d,h). This can be explained through the compensating effects of rising TA
588 and changing P on plant productivity and ecosystem respiration. For instance, MIROC5 and
589 AVE exhibit similar values of TA that were both larger than HIST (Fig. 6c), but there is a larger
590 summer P in MIROC5 as compared to both AVE and HIST (which have similar totals, Fig. 6d).
591 While rising TA increases evaporative demand, higher P reduces soil moisture stress. The net
592 result is an increase in GPP and NEP in MIROC5 relative to AVE, whereas MIROC5 and HIST

593 are fairly close with respect to summer season carbon fluxes. This suggests that higher summer P
594 has the capacity to compensate for increased summer TA (MIROC5 vs. HIST), while
595 maintaining similar precipitation under rising temperature leads to a lower GPP and NEP (AVE
596 vs. HIST). This latter case is consistent with experimental studies where increased temperatures
597 have been shown to unfavorably affect productivity under constant precipitation treatments (e.g.
598 Epstein et al., 1997; Mowll et al., 2015; Wu et al., 2011). Moreover, large increases in TA along
599 with decreases in P, like the HadGEM2-ES scenario, significantly decrease GPP in the
600 subtropical shrubland such that there is a collapse in the simulated plant activity. As a result,
601 increased summertime air temperatures and reduced precipitation could cause large impacts on
602 vegetation productivity that would require further plant adaptations or variations in community
603 composition, as suggested in prior work (Dieleman et al., 2015; Goyal, 2004; Lavee et al., 1998;
604 Moritz & Agudo, 2013; Ponce Campos et al., 2013; Schwinning & Ehleringer, 2001).

605 A closer inspection of the summer carbon fluxes in Fig. 8 reveals substantial variations
606 between pre-monsoon (MJ) and monsoon (JAS) periods in the scenarios (HadGEM2-ES is
607 omitted as GPP approached zero after 35 years of simulation) as well as the relative importance
608 of heterotrophic (R_h) and ecosystem respiration (R_{ECO}) on net ecosystem productivity. For all
609 scenarios, pre-monsoon magnitudes of R_h and R_{ECO} were smaller than respiration fluxes during
610 the monsoon, consistent with the drier soil conditions and lower microbial biomass (Fig. 8a, b),
611 as presented in other sites in the NAM region (Barron-Gafford et al., 2012). Furthermore, R_h is a
612 larger fraction of R_{ECO} for the pre-monsoon period ($R_h/R_{ECO} = 0.53, 0.52, 0.51$ and 0.55 for
613 HIST, CNRM-CM5, MIROC5 and AVE) as compared to monsoon conditions ($R_h/R_{ECO} = 0.32,$
614 $0.31, 0.33$ and 0.34), indicating that R_a increases in importance during the summer. Variations in
615 monsoon values of respiration fluxes across the scenarios follow patterns in gross primary

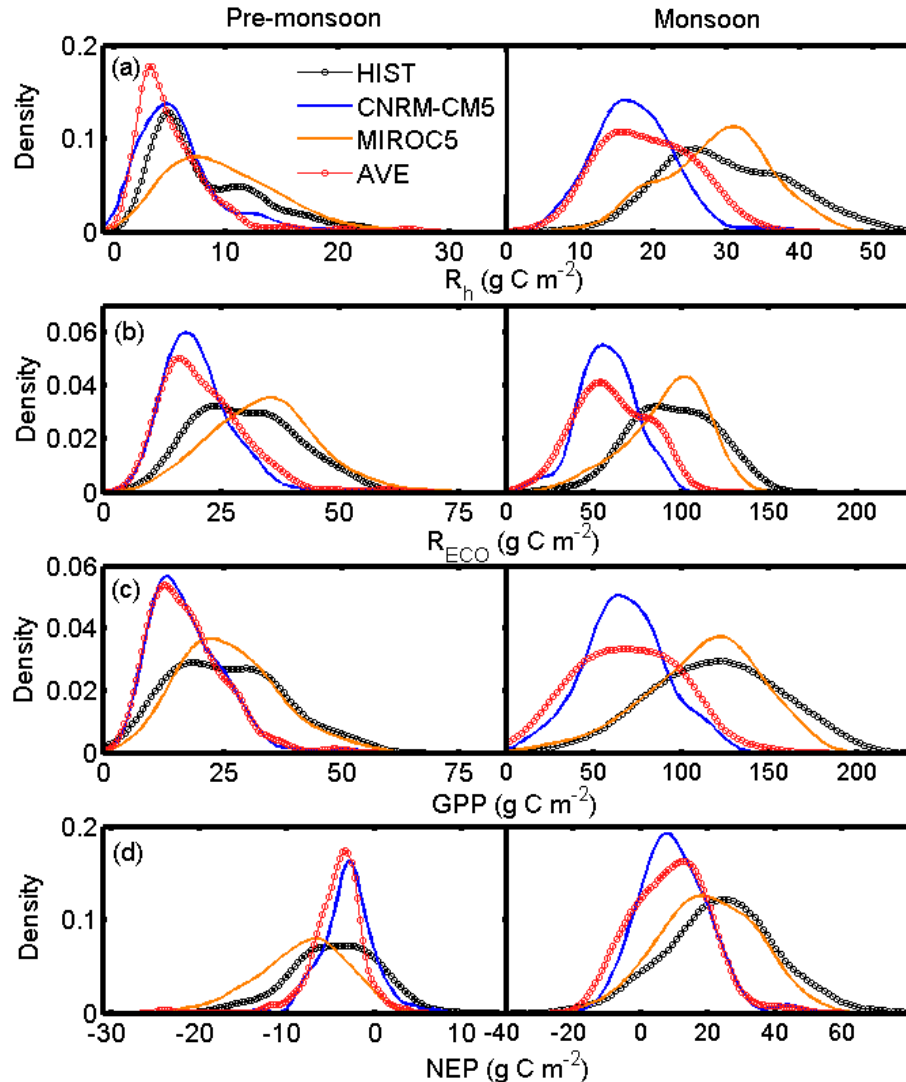
616 productivity (Fig. 7g), as shown in prior studies (Gómez-Casanovas et al., 2012; Stoy et al.,
617 2009). For example, R_h was correlated well with GPP ($R^2 > 0.60$, $p < 0.05$) such that scenarios
618 with a higher GPP (HIST and MIROC5) exhibit higher R_h due to the increased availability of
619 litterfall for decomposition (Fig. 8b,c). In contrast, pre-monsoon periods showed sensitivity to
620 both GPP and SWC such that MIROC5 with a higher P had substantially larger R_h than those
621 scenarios with similar TA but lower P. This is consistent with other studies indicating that
622 productivity enhancements via water availability are more critical controls on respiration than air
623 temperature changes in semiarid ecosystems (Janssens et al., 2001; Reichstein et al., 2003). Pre-
624 monsoon conditions also had substantially lower GPP and NEP as compared to the monsoon
625 period (Fig. 8c,d), with more negative values of NEP indicating the relative importance of R_{ECO}
626 as compared to GPP prior to the growing season. Furthermore, higher precipitation and rising air
627 temperatures (MIROC5) promote a more substantial R_h that reduce NEP, whereas a lower P and
628 higher TA (CNRM-CM5 and AVE) resulted in NEP closer to zero. As result, subtropical
629 shrublands could become a larger net carbon source during pre-monsoon periods when warming
630 is coupled with increased precipitation.

631 **3.4. CO₂ fertilization effects on simulated water, energy and carbon dynamics**

633 Superimposed effects of meteorological changes and increased atmospheric CO₂
634 concentrations (482 ppm over the 2030-2045 period) were assessed using a second set of
635 simulations for each model scenario (CNRM-CM5, HadGEM2-ES, MIROC5 and AVE). Fig. 9
636 presents the modeling outcomes for the climate change experiments (with and without CO₂
637 fertilization) relative to the HIST (1990-2005) simulation and the summer (MJJAS) averaged
638 observations (OBS, 2008-2012). Differences between HIST and OBS were only due to the
639 sampling of different time periods since simulations during 2008-2012 were consistent with OBS

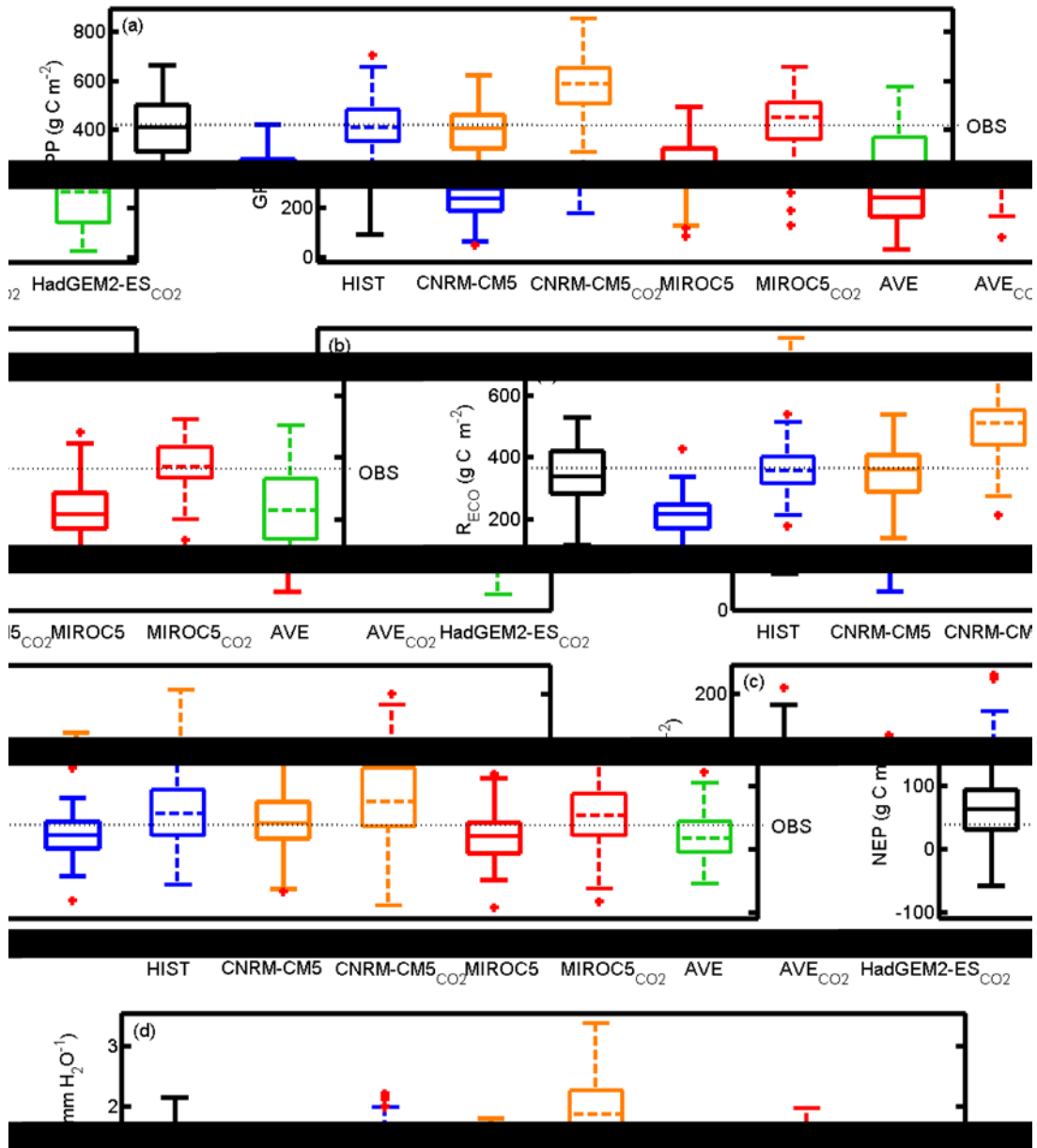
640 (Table 4). For the higher CO₂ scenarios, both GPP (+172.1, 188.5 and 210.5 g C m⁻² for CNRM-
641 CM5, MIROC5 and AVE, respectively) and R_{ECO} (+146.9, 147.0 and 153.7 g C m⁻²) show
642 increases when compared to the CO₂ of 365 ppm case (Fig. 9a, b). Thus, for the same set of
643 imposed meteorological changes, increased atmospheric CO₂ enhances GPP, as seen in field and
644 remote sensing studies (Ainsworth & Long, 2005; Donohue et al., 2013; Morgan et al., 2004;
645 Wang et al., 2012), and that is consistent with higher observed ecosystem respiration. Larger
646 enhancements in GPP and R_{ECO} were noted for scenarios with more precipitation during the
647 summer (MIROC5 vs. CNRM-CM5). However, the increase in GPP due to CO₂ fertilization
648 exceeds that of R_{ECO} due to a reduction of the autotrophic respiration per unit leaf area (e.g.
649 Drake et al., 1997). As a result, NEP from the CO₂ fertilization experiments increased in terms of
650 the median value and the range of values in all scenarios relative to simulations without a rising
651 CO₂ (Fig. 9c). Thus, CO₂ fertilization offsets the meteorological impacts on NEP in the near-
652 future (2030-2045) at the expense of an increase summer interannual variability. The positive
653 effects of fertilization on the median NEP varied across the scenarios (+34.6, 33.2 and 33.9 g C
654 m⁻²) with a higher increase for AVE with the largest increase in WUE. In addition, the CO₂
655 fertilization altered NEP at the subtropical shrubland under the HadGEM2-ES scenario
656 permitting ecosystem resilience and a positive carbon balance.

657 The role of precipitation changes on enhancing NEP was further explored by comparing
658 SWC for the two sets of CO₂ experiments. As expected, higher GPP for scenarios with CO₂
659 fertilization was linked to a dramatic increase in LAI (+72%, 45% and 73% for CNRM-CM5,
660 MIROC5 and AVE, respectively) relative to the cases with CO₂ at 365 ppm, which resulted in a
661 higher summertime ET (+18, 13 and 21 mm). While the higher ET under CO₂ fertilization would



662
 663 **Figure 8.** Comparison of carbon dynamics for historical (1990-2005) and climate change
 664 experiments (2030-2045) using representative realizations for HIST, CNRM-CM5, MIROC5 and
 665 AVE for pre-monsoon (MJ) and monsoon (JAS) periods. Probability density functions of (a)
 666 heterotrophic respiration (R_h), (b) ecosystem respiration (R_{ECO}), (c) gross primary productivity
 667 (GPP) and (d) net ecosystem productivity (NEP) totals during each period.

668
 669 be expected to deplete soil water, we found no appreciable changes in SWC of the top 10 cm of
 670 soil (+0.0013, 0.0007 and 0.0019 m^3/m^3), even for cases where summertime precipitation
 671 decreased or remained similar (CNRM-CM5 and AVE). These results are consistent with Fatichi
 672 et al. (2016a) who showed that increased WUE supports a higher LAI through soil water savings
 673 but leads to a more rapid consumption of SWC due to the increased vegetation. The effects of



674
675
676
677
678
679
680
681
682
683
684

Figure 9. Box-whisker plots of summer (MJJAS) R_{ECO} , GPP, NEP and WUE for the climate change experiments under meteorological changes and superimposed CO_2 fertilization (labeled with subscript CO_2) using representative realizations for HIST, CNRM-CM5, HadGEM2-ES, MIROC5 and AVE. Dashed horizontal line in each subplots represents summer averages from observations (OBS, 2008-2012).

increased CO_2 on gains in NEP despite a similar SWC when compared to scenarios without fertilization is attributed to ecosystem alterations in water use efficiency ($WUE = GPP/ET$, Fig. 9d), which increased substantially (+68%, 42% and 69%) at the expense of higher summertime interannual variability. Thus, a secondary effect of CO_2 fertilization is to allow more productive

685 summers (i.e. higher NEP), when precipitation is not limiting, through higher WUE. As a result,
686 CO₂ fertilization leads to a more efficient but variable ecosystem in terms of biomass production
687 per amount of water consumed in most of the scenarios. Prior investigations have identified
688 similar CO₂ fertilization effects on WUE, including through experimental studies of semiarid
689 plants (e.g. Leakey et al., 2009, Morgan et al., 2011, Xu et al., 2014) and analyses of remotely-
690 sensed data in drylands (e.g. Donohue et al., 2013, Lu et al., 2016). Nevertheless, it has been
691 uncommon to measure WUE directly in semiarid regions with strong vegetation dynamics. As
692 such, there is a need to conduct additional observational analyses in seasonally-dry ecosystems to
693 compare with our model-based estimates of the CO₂ fertilization effect on WUE (+40% to 70%),
694 as have been performed in temperate forests (Kauwe et al., 2013). In our study, the increase in
695 WUE was greater in the warmest scenario (HadGEM2-ES) since elevated CO₂ allows plants to
696 decrease stomatal conductance, while maintaining photosynthetic rates (Blumenthal et al., 2013),
697 which resulted in positive NEP under CO₂ fertilization. Similar effects have been observed under
698 experimental CO₂ fertilization (e.g. Cernusak et al., 2013; Conley et al., 2001) and more recently
699 as a trend due to rising CO₂ concentrations (e.g. Maseyk et al., 2011; Lu et al., 2016).

700

701 **4. Summary and conclusions**

702 In this work, we combined ecohydrological and soil carbon models to simulate water,
703 energy and carbon dynamics in a seasonally-dry, semiarid ecosystem of northwestern México
704 across temporal resolutions ranging from hourly to interannual variability. Compared to a set of
705 field and remotely-sensed observations, the tRIBS-VEGGIE and SCM simulations accurately
706 captured the seasonality of vegetation activity and carbon fluxes of subtropical shrublands
707 (Méndez-Barroso et al., 2014; Villarreal et al., 2016; Vivoni et al., 2010a). In addition, the
708 simulations represent the main features of net primary productivity in the region, specifically a

709 large respiration pulse early in the summer followed by a gradual switch to carbon fixation
710 during the growing season (Huxman et al., 2004b; Verduzco et al., 2015; Yépez et al., 2007).
711 This indicated that the simulation of soil (heterotrophic) respiration is an essential component for
712 reproducing the observed carbon dynamics in this type of ecosystem. Furthermore, simulated R_h
713 was highly sensitive to timing of the first storms during the NAM that increase soil water content
714 and to the amount of labile substrate derived from litterfall from the previous summer. Insights
715 gained from the ecohydrological and soil carbon model application could potentially serve to
716 improve terrestrial biosphere models (e.g. Huntzinger et al., 2012) that have been shown to
717 misrepresent carbon dynamics in semiarid shrublands. Nevertheless, the use of the combined
718 models within this ecosystem could be improved by adding a plant functional type, such as
719 winter annuals (Werk et al., 1983) or evergreen shrubs (Biederman et al., 2018), that is active
720 from fall to spring. In this manner, the physiological activity during winters would enhance the
721 representation of vegetation dynamics and impact the generation and decomposition of litterfall,
722 thus affecting the respiratory efflux at the start of the following monsoon. This is consistent with
723 Verduzco et al. (2015) and Zhang et al. (2014) who suggested the net carbon balance depends on
724 the relative strength of the heterotrophic carbon release versus the primary productivity occurring
725 later in the growing season. Overall, both the observed record and simulations over the studied
726 (2008-2012) and historical (1990-2005) periods showed that the subtropical shrubland was
727 generally a net carbon sink (positive NEP) over both growing season and annual time scales.

728 Subsequently, we conducted a comparison of historical (1990-2005) and near-future
729 (2030-2045) climate change scenarios obtained from the stochastic downscaling of three GCMs
730 (Fatichi et al., 2011, 2013) tailored for input to the tRIBS-VEGGIE and SCM models. Increased
731 near-future air temperatures reduced net ecosystem productivity, though a compensation effect

732 was identified for some of GCMs (e.g., MIROC5) exhibiting higher summer precipitation as
733 compared to the historical scenario (HIST). This was attributed to higher plant stress under
734 warmer temperatures and lower precipitation, which limited GPP. Since R_{ECO} was reduced to a
735 lesser degree than GPP, due to warmer temperatures and short-term substrate availability, a
736 lower NEP resulted in all scenarios, with compensation occurring when atmospheric CO_2
737 concentration was increased. When GCM projections of summer precipitation were substantially
738 lower (HadGEM2-ES), a collapse of the simulated plant activity was observed (i.e. GPP
739 approaching zero). It should be noted, however, that tRIBS-VEGGIE simulations do not
740 currently account for plant thermal acclimation that can prevent ‘diebacks’ due to high
741 temperatures (Hamerlynck et al., 2000; Salvucci & Crafts-Brandner, 2004) or for plant mortality
742 processes induced by cavitation (Fatichi et al., 2016b; Plaut et al., 2012), and thus the collapse of
743 plant activity under the HadGEM2-ES scenario is subject to considerable uncertainty.

744 Our main finding was that reductions in NEP under near-future meteorological changes
745 were significantly offset under the CO_2 fertilization experiments for all considered GCMs. This
746 was mainly attributed to an increase in WUE under elevated CO_2 concentrations via an indirect
747 effect on SWC as identified in other water-limited ecosystems (Fatichi et al., 2016b; Lu et al.,
748 2016). As a result of higher soil water content, the effects of warming-induced stress can be
749 offset, leading to increases in NEP in the near-future for all GCMs relative to the historical
750 period. Increases in WUE under CO_2 fertilization help to explain how seasonally-dry ecosystems
751 can recover as a net carbon sink with a strength similar to the historical conditions under the
752 superimposed climate change effects. For the scenario with higher summer precipitation
753 (MIROC5), near-future NEP is larger than HIST, whereas for the case with the highest summer
754 temperature (HadGEM2-ES), CO_2 fertilization prevents the collapse of the simulated plant

755 activity. Nevertheless, these projected changes are also subject to uncertainty since
756 photosynthetic acclimation to elevated CO₂ (Newingham et al., 2013; Mueller et al., 2016; Sage
757 et al., 1989) is not currently considered.

758 Given the important role of semiarid regions in the terrestrial carbon budget (Ahlström et
759 al., 2015; Poulter et al., 2014), the effects of meteorological changes and CO₂ fertilization on
760 carbon dynamics in seasonally-dry ecosystems could have regional to global consequences.
761 Under warming conditions, lower precipitation and increased atmospheric CO₂, our study
762 suggests that semiarid ecosystems under the influence of the North American monsoon would
763 maintain a similar to actual net carbon balance by mid 21st century. The offsetting of impacts
764 from meteorological changes in temperature and precipitation and those arising from CO₂
765 fertilization is an outcome of opposing controls on soil and plant-mediated carbon dynamics.
766 However, changes in the timing, intensity and distribution of precipitation during the growing
767 season (e.g. Cook & Seager, 2013; Geil et al., 2013), in particular an increase in monsoon
768 rainfall (e.g. Hawkins et al., 2015; Robles-Morua et al., 2015), could lead to ecosystems acting as
769 larger net carbon sinks, due to an increase in water use efficiency under higher CO₂
770 concentrations, with implications on the global carbon budget. This outcome is consistent with
771 observed biomass trends indicating more efficient productivity in semiarid ecosystems (Donahue
772 et al., 2013), including those in the NAM region (Forzieri et al., 2014). While additional research
773 is necessary to confirm the findings of this study and their implications for terrestrial biosphere
774 models used to capture feedbacks to the climate system (Huntzinger et al., 2012), the combined
775 use of dynamic ecosystem level measurements and numerical modeling is a promising avenue
776 for deciphering the net effect of climate change on the water, energy and carbon dynamics of
777 seasonally-dry, semiarid ecosystems.

778

779 **Acknowledgments**

780 We thank the Consejo Nacional de Ciencia y Tecnología (CONACYT) in México for the
781 graduate fellowship to V.S.V. (231560) and T.T. (232184). This research project was supported
782 by CB-2013-01: 221014 to E.A.Y. and a US Fulbright and CONACYT Visiting Fellowships to
783 E.R.V. We also thank the World Climate Research Programme's Working Group on Coupled
784 Modelling, for producing and making available the climate change model output. We thank two
785 reviewers for excellent comments that helped to improve an earlier version of the manuscript.
786 Data access is available through Zenodo at <http://doi.org/10.5281/zenodo.1116422> and the model
787 code and outputs utilized in this study can be requested from the corresponding author.

788 **References**

- 789 Ahlström, A., Raupach, M. R., Schurgers, G., Smith, B., Arneth, A., Jung, M., ... & Kato, E.
790 (2015). The dominant role of semi-arid ecosystems in the trend and variability of the land
791 CO₂ sink. *Science*, 348(6237), 895-899. [https://doi.org/ 10.1126/science.aaa1668](https://doi.org/10.1126/science.aaa1668)
792 Ainsworth, E. A., & Long, S. P. (2005). What have we learned from 15 years of free-air CO₂
793 enrichment (FACE)? A meta-analytic review of the responses of photosynthesis, canopy
794 properties and plant production to rising CO₂. *New Phytologist*, 165(2), 351-372.
795 <https://doi.org/10.1111/j.1469-8137.2004.01224.x>.
796 Allard, V., Ourcival J.M., Rambal S., Joffre R., Rocheteau A. (2008). Seasonal and annual
797 variation of carbon exchange in an evergreen Mediterranean forest in southern
798 France. *Global Change Biology*, 14(4), 714-725. <https://doi.org/10.1111/j.1365-2486.2008.01539.x>
800 Amthor, J.S. (1984) The role of maintenance respiration in plant growth. *Plant, Cell &*
801 *Environment*, 7(8), 561-569. <https://doi.org/10.1111/1365-3040.ep11591833>
802 Anderson, C. A., & Vivoni, E. R. (2016) Impact of land surface states within the flux footprint
803 on daytime land-atmosphere coupling in two semiarid ecosystems of the Southwestern
804 US. *Water Resources Research*, 52(6), 4785-4800.
805 <https://doi.org/10.1002/2015WR018016>
806 Arnone Iii, J. A., Verburg, P. S., Johnson, D. W., Larsen, J. D., Jasoni, R. L., Lucchesi, A. J., ...
807 & Buck, P. E. (2008) Prolonged suppression of ecosystem carbon dioxide uptake after an
808 anomalously warm year. *Nature*, 455(7211), 383-386.
809 <http://doi.org/10.1038/nature07296>
810 Aubinet, M., Grelle, A., Ibrom, A., Rannik, Ü., Moncrieff, J., Foken, T., ... & Clement, R. (2000)
811 Estimates of the annual net carbon and water exchange of forests: The EUROFLUX
812 methodology. *Advances in Ecological Research*, 30, 113-175.
813 [https://doi.org/10.1016/S0065-2504\(08\)60018-5](https://doi.org/10.1016/S0065-2504(08)60018-5)
814 Babst, F., Bouriaud, O., Papale, D., Gielen, B., Janssens, I. A., Nikinmaa, E., ... & Grünwald, T.
815 (2014) Above-ground woody carbon sequestration measured from tree rings is coherent
816 with net ecosystem productivity at five eddy-covariance sites. *New Phytologist*, 201(4),
817 1289-1303. <https://doi.org/10.1111/nph.12589>
818 Baldocchi, D., Falge, E., Gu, L., Olson, R., Hollinger, D., Running, S., ... & Fuentes, J. (2001).
819 FLUXNET: A new tool to study the temporal and spatial variability of ecosystem-scale
820 carbon dioxide, water vapor, and energy flux densities. *Bulletin of the American*
821 *Meteorological Society*, 82(11), 2415-2434. [https://doi.org/10.1175/1520-0477\(2001\)082<2415:FANTTS>2.3.CO;2](https://doi.org/10.1175/1520-0477(2001)082<2415:FANTTS>2.3.CO;2)
822
823 Baldocchi, D. D. (2003). Assessing the eddy covariance technique for evaluating carbon dioxide
824 exchange rates of ecosystems: past, present and future. *Global Change biology*, 9(4),
825 479-492. [https://doi.org/ 10.1046/j.1365-2486.2003.00629.x](https://doi.org/10.1046/j.1365-2486.2003.00629.x)
826 Baldocchi, D.D. (2008). 'Breathing' of the terrestrial biosphere: lessons learned from a global
827 network of carbon dioxide flux measurement systems. *Australian Journal of*
828 *Botany*, 56(1), 1-26. <https://doi.org/10.1071/BT07151>
829 Barr, A. G., Richardson, A. D., Hollinger, D. Y., Papale, D., Arain, M. A., Black, T. A., ... &
830 Law, B. E. (2013). Use of change-point detection for friction-velocity threshold
831 evaluation in eddy-covariance studies. *Agricultural and Forest Meteorology*, 171, 31-45.
832 <https://doi.org/10.1016/j.agrformet.2012.11.023>

833 Barron-Gafford, G. A., Scott, R. L., Jenerette, G. D., Hamerlynck, E. P., & Huxman, T. E.
834 (2012). Temperature and precipitation controls over leaf-and ecosystem-level CO₂ flux
835 along a woody plant encroachment gradient. *Global Change Biology*, 18(4), 1389-1400.
836 10.1111/j.1365-2486.2011.02599.x

837 Biederman, J. A., Scott, R. L., Goulden, M. L., Vargas, R., Litvak, M. E., Kolb, T. E., ... &
838 Garatuza-Payan, J. (2016). Terrestrial carbon balance in a drier world: the effects of water
839 availability in southwestern North America. *Global Change Biology*, 22(5), 1867-1879.
840 <https://doi.org/10.1111/gcb.13222>

841 Biederman, J. A., Scott, R. L., Bell, T., Bowling, D., Dore, S., Garatuza-Payan, J., Kolb, T.,
842 Kirishnan, P., Krofcheck, D., Litvak, M., Maurer, G., Meyers, T., Oechel, W., Papuga, S.,
843 Ponce Campos, G. E., Rodriguez, J., Smith, W., Vargas, E., Watts, C., Yezpez, E., &
844 Goulden, M. (2017). CO₂ exchange and evapotranspiration across dryland ecosystems of
845 southwestern North America. *Global Change Biology*, 23, 4204-4221.
846 <https://doi.org/10.1111/gcb.13686>.

847 Biederman, J. A., Scott, R. L., Arnone, J., Jasoni, R. L., Litvak, M. E., Moreo, M. T., Papuga, S.
848 A., Ponce-Campos, G. E., Schreiner-McGraw, A. P., & Vivoni, E.R. (2018). Shrubland
849 carbon sink depends upon winter water availability in the warm deserts of North
850 America. *Agricultural and Forest Meteorology*, 249, 407-419.
851 <https://doi.org/10.1016/j.agrformet.2017.11.005>

852 Blumenthal, D. M., Resco, V., Morgan, J. A., Williams, D. G., LeCain, D. R., Hardy, E. M., ... &
853 Bladyka, E. (2013). Invasive forb benefits from water savings by native plants and carbon
854 fertilization under elevated CO₂ and warming. *New Phytologist*, 200(4), 1156-1165.
855 <https://doi.org/10.1111/nph.12459>

856 Bolker, B. M., Pacala, S. W., & Parton, W. J. (1998). Linear analysis of soil decomposition:
857 insights from the century model. *Ecological Applications*, 8(2), 425-439.
858 [https://doi.org/10.1890/1051-0761\(1998\)008\[0425:LAOSDI\]2.0.CO;2](https://doi.org/10.1890/1051-0761(1998)008[0425:LAOSDI]2.0.CO;2)

859 Bolton, H., Smith, J. L., & Link, S. O. (1993). Soil microbial biomass and activity of a disturbed
860 and undisturbed shrub-steppe ecosystem. *Soil Biology and Biochemistry*, 25(5), 545-552.
861 [https://doi.org/10.1016/0038-0717\(93\)90192-E](https://doi.org/10.1016/0038-0717(93)90192-E)

862 Brown, DE (1994) *Biotic Communities: Southwestern United States and Northwestern México*.
863 University of Utah Press, Salt Lake City, UT.

864 Búrquez, A., Martínez-Yrizar, A., & Núñez, S. (1999). Sonoran Desert productivity and the
865 effect of trap size on litterfall estimates in dryland vegetation. *Journal of Arid*
866 *Environments*, 43(4), 459-465. <https://doi.org/10.1006/jare.1999.0547>

867 Cable, J. M., Ogle, K., Williams, D. G., Weltzin, J. F., & Huxman, T. E. (2008). Soil texture
868 drives responses of soil respiration to precipitation pulses in the Sonoran Desert:
869 implications for climate change. *Ecosystems*, 11(6), 961-979.
870 <https://doi.org/10.1007/s10021-008-9172-x>

871 Carbone, M. S., Still, C. J., Ambrose, A. R., Dawson, T. E., Williams, A. P., Boot, C. M., ... &
872 Schimel, J. P. (2011). Seasonal and episodic moisture controls on plant and microbial
873 contributions to soil respiration. *Oecologia*, 167(1), 265-278.
874 <https://doi.org/10.1007/s00442-011-1975-3>

875 Carbone, M. S., Richardson, A. D., Chen, M., Davidson, E. A., Hughes, H., Savage, K. E., &
876 Hollinger, D. Y. (2016). Constrained partitioning of autotrophic and heterotrophic
877 respiration reduces model uncertainties of forest ecosystem carbon fluxes but not

878 stocks. *Journal of Geophysical Research: Biogeosciences*, 121(9), 2476-2492.
879 <https://doi.org/10.1002/2016JG003386>

880 Cardoso, J. A. F., Lima, A. M. N., Cunha, T. J. F., Rodrigues, M. S., Hernani, L. C., Amaral, A.
881 J. D., & Oliveira Neto, M. B. D. (2015). Organic matter fractions in a Quartzipsamment
882 under cultivation of irrigated Mmango in the Lower São Francisco valley region,
883 Brazil. *Revista Brasileira de Ciência do Solo*, 39(4), 1068-1078.
884 <https://dx.doi.org/10.1590/01000683rbc20140498>

885 Castro, C. L., Chang, H. I., Dominguez, F., Carrillo, C., Schemm, J. K., & Henry Juang, H. M.
886 (2012). Can a regional climate model improve the ability to forecast the North American
887 monsoon?. *Journal of Climate*, 25(23), 8212-8237. [https://doi.org/10.1175/JCLI-D-11-](https://doi.org/10.1175/JCLI-D-11-00441.1)
888 [00441.1](https://doi.org/10.1175/JCLI-D-11-00441.1)

889 Cerezo-Mota, R., Allen, M., & Jones, R. (2011). Mechanisms controlling precipitation in the
890 northern portion of the North American monsoon. *Journal of Climate*, 24(11), 2771-
891 2783. <https://doi.org/10.1175/2011JCLI3846.1>

892 Cernusak, L. A., Winter, K., Dalling, J. W., Holtum, J. A., Jaramillo, C., Körner, C., ... &
893 Wright, S. J. (2013). Tropical forest responses to increasing atmospheric CO₂: current
894 knowledge and opportunities for future research. *Functional Plant Biology*, 40(6), 531-
895 551. <https://doi.org/10.1071/FP12309>

896 Collins, S. L., Belnap, J., Grimm, N. B., Rudgers, J. A., Dahm, C. N., D'odorico, P., ... &
897 Sinsabaugh, R. L. (2014). A multiscale, hierarchical model of pulse dynamics in arid-land
898 ecosystems. *Annual Review of Ecology, Evolution, and Systematics*, 45, 397-419.
899 <https://doi.org/10.1146/annurev-ecolsys-120213-091650>

900 Conant, R. T., Dalla-Betta, P., Klopatek, C. C., & Klopatek, J. M. (2004). Controls on soil
901 respiration in semiarid soils. *Soil Biology and Biochemistry*, 36(6), 945-951.
902 <https://doi.org/10.1016/j.soilbio.2004.02.013>

903 Conley, M. M., Kimball, B. A., Brooks, T. J., Pinter, P. J., Hunsaker, D. J., Wall, G. W., ... &
904 Leavitt, S. W. (2001). CO₂ enrichment increases water-use efficiency in sorghum. *New*
905 *Phytologist*, 151(2), 407-412. <https://doi.org/10.1046/j.1469-8137.2001.00184.x>

906 Cook, B. I., & Seager, R. (2013). The response of the North American Monsoon to increased
907 greenhouse gas forcing. *Journal of Geophysical Research: Atmospheres*, 118(4), 1690-
908 1699. <https://doi.org/10.1002/jgrd.50111>

909 Cheng, M., Xue, Z., Xiang, Y., Darboux, F., & An, S. (2015). Soil organic carbon sequestration
910 in relation to revegetation on the Loess Plateau, China. *Plant and Soil*, 397(1-2), 31-42.
911 <https://doi.org/10.1007/s11104-015-2486-5>

912 Davidson, E. A., Janssens, I. A., & Luo, Y. (2006). On the variability of respiration in terrestrial
913 ecosystems: moving beyond Q₁₀. *Global Change Biology*, 12(2), 154-164.
914 <https://doi.org/10.1111/j.1365-2486.2005.01065.x>

915 Desai, A. R., Richardson, A. D., Moffat, A. M., Kattge, J., Hollinger, D. Y., Barr, A., ... &
916 Stauch, V. J. (2008). Cross-site evaluation of eddy covariance GPP and RE
917 decomposition techniques. *Agricultural and Forest Meteorology*, 148(6), 821-838.
918 <https://doi.org/10.1016/j.agrformet.2007.11.012>

919 Dieleman, C. M., Branfireun, B. A., McLaughlin, J. W., & Lindo, Z. (2015). Climate change
920 drives a shift in peatland ecosystem plant community: implications for ecosystem
921 function and stability. *Global Change Biology*, 21(1), 388-395.
922 <https://doi.org/10.1111/gcb.12643>

- 923 Donohue, R. J., Roderick, M. L., McVicar, T. R., & Farquhar, G. D. (2013). Impact of CO₂
924 fertilization on maximum foliage cover across the globe's warm, arid
925 environments. *Geophysical Research Letters*, *40*(12), 3031-3035.
926 <https://doi.org/10.1002/grl.50563>
- 927 Douglas, M. W., Maddox, R. A., Howard, K., & Reyes, S. (1993). The mexican
928 monsoon. *Journal of Climate*, *6*(8), 1665-1677. [https://doi.org/10.1175/1520-0442\(1993\)006<1665:TMM>2.0.CO;2](https://doi.org/10.1175/1520-0442(1993)006<1665:TMM>2.0.CO;2)
- 929
930 Drake, B. G., González-Meler, M. A., & Long, S. P. (1997). More efficient plants: a
931 consequence of rising atmospheric CO₂?. *Annual Reviews of Plant Biology*, *48*(1), 609-
932 639. <https://doi.org/10.1146/annurev.arplant.48.1.609>
- 933 Drake, J. E., Aspinwall, M. J., Pfautsch, S., Rymer, P. D., Reich, P. B., Smith, R. A., ... &
934 Tjoelker, M. G. (2015). The capacity to cope with climate warming declines from
935 temperate to tropical latitudes in two widely distributed Eucalyptus species. *Global*
936 *Change Biology*, *21*(1), 459-472. <https://doi.org/10.1111/gcb.12729>
- 937 Duan, Q. Y., Gupta, V. K., & Sorooshian, S. (1993). Shuffled complex evolution approach for
938 effective and efficient global minimization. *Journal of Optimization Theory and*
939 *Applications*, *76*, 501-521. <https://doi.org/10.1007/BF00939380>
- 940 Duarte, H. F., Dias, N. L., & Maggiotto, S. R. (2006). Assessing daytime downward longwave
941 radiation estimates for clear and cloudy skies in Southern Brazil. *Agricultural and Forest*
942 *Meteorology*, *139*(3), 171-181. <https://doi.org/10.1016/j.agrformet.2006.06.008>
- 943 Duursma, R. A., Barton, C. V. M., Lin, Y-S., Medlyn, B. E., Eamus, D., Tissue, D. T., Ellsworth,
944 D. S., and McMurthie, R. E. (2014). The peaked response of transpiration rate to vapour
945 pressure deficit in field conditions can be explained by the temperature optimum of
946 photosynthesis. *Agricultural and Forest Meteorology*, *189-190*: 2-10.
947 <https://doi.org/10.1016/j.agrformet.2013.12.007>
- 948 Epstein, H. E., Lauenroth, W. K., & Burke, I. C. (1997). Effects of temperature and soil texture
949 on ANPP in the US Great Plains. *Ecology*, *78*(8), 2628-2631.
950 [https://doi.org/10.1890/0012-9658\(1997\)078\[2628:EOTAST\]2.0.CO;2](https://doi.org/10.1890/0012-9658(1997)078[2628:EOTAST]2.0.CO;2)
- 951 Euskirchen, E. S., Edgar, C. W., Turetsky, M. R., Waldrop, M. P., & Harden, J. W. (2014).
952 Differential response of carbon fluxes to climate in three peatland ecosystems that vary in
953 the presence and stability of permafrost. *Journal of Geophysical Research:*
954 *Biogeosciences*, *119*(8), 1576-1595. <https://doi.org/10.1002/2014JG002683>
- 955 Fan, J., Jones, S. B., Qi, L. B., Wang, Q. J., & Huang, M. B. (2012). Effects of precipitation
956 pulses on water and carbon dioxide fluxes in two semiarid ecosystems: measurement and
957 modeling. *Environmental Earth Sciences*, *67*(8), 2315-2324.
958 <https://doi.org/10.1007/s12665-012-1678-z>
- 959 Fatichi, S., Ivanov, V. Y., & Caporali, E. (2013). Assessment of a stochastic downscaling
960 methodology in generating an ensemble of hourly future climate time series. *Climate*
961 *Dynamics*, *40*(7-8), 1841-1861. <https://doi.org/10.1007/s00382-012-1627-2>
- 962 Fatichi, S., Ivanov, V. Y., & Caporali, E. (2011). Simulation of future climate scenarios with a
963 weather generator. *Advances in Water Resources*, *34*(4), 448-467.
964 <https://doi.org/10.1016/j.advwatres.2010.12.013>
- 965 Fatichi, S., Leuzinger, S., Paschalis, A., Langley, J. A., Barraclough, A. D., & Hovenden, M. J.
966 (2016). Partitioning direct and indirect effects reveals the response of water-limited
967 ecosystems to elevated CO₂. *Proceedings of the National Academy of Sciences*, *113*(45),
968 12757-12762. <https://doi.org/10.1073/pnas.1605036113>

- 969 Fatichi, S., Pappas, C., & Ivanov, V. Y. (2016b). Modeling plant–water interactions: an
970 ecohydrological overview from the cell to the global scale. *Wiley Interdisciplinary*
971 *Reviews: Water*, 3(3), 327-368. <https://doi.org/10.1002/wat2.1125>
- 972 Fensholt, R., Sandholt, I., & Rasmussen, M. S. (2004). Evaluation of MODIS LAI, fAPAR and
973 the relation between fAPAR and NDVI in a semi-arid environment using in situ
974 measurements. *Remote Sensing of Environment*, 91(3), 490-507.
975 <https://doi.org/10.1016/j.rse.2004.04.009>
- 976 Fisher, J. B., Huntzinger, D. N., Schwalm, C. R., & Sitch, S. (2014). Modeling the terrestrial
977 biosphere. *Annual Reviews of Environment and Resources*, 39, 91-123.
978 <https://doi.org/10.1146/annurev-environ-012913-093456>
- 979 Flanagan, L. B., Wever, L. A., & Carlson, P. J. (2002). Seasonal and interannual variation in
980 carbon dioxide exchange and carbon balance in a northern temperate grassland. *Global*
981 *Change Biology*, 8(7), 599-615. <https://doi.org/10.1046/j.1365-2486.2002.00491.x>
- 982 Flato, G., Marotzke, J., Abiodun, B., Braconnot, P., Chou, S. C., Collins, W. J., ... & Forest, C.
983 (2013). Evaluation of Climate Models. In: Climate Change 2013: The Physical Science
984 Basis. Contribution of Working Group I to the Fifth Assessment Report of the
985 Intergovernmental Panel on Climate Change. *Climate Change 2013*, 5, 741-
986 866. <https://doi.org/10.1017/CBO9781107415324.020>
- 987 Follett, R. F., Paul, E. A., & Pruessner, E. G. (2007). Soil carbon dynamics during a long-term
988 incubation study involving ¹³C and ¹⁴C measurements. *Soil Science*, 172(3), 189-208.
989 <https://doi.org/10.1097/ss.0b013e31803403de>
- 990 Forzieri, G., Feyen, L., Cescatti, A., & Vivoni, E. R. (2014). Spatial and temporal variations in
991 ecosystem response to monsoon precipitation variability in southwestern North
992 America. *Journal of Geophysical Research: Biogeosciences*, 119(10), 1999-2017.
993 <https://doi.org/10.1002/2014JG002710>
- 994 Friedlingstein, P., Meinshausen, M., Arora, V. K., Jones, C. D., Anav, A., Liddicoat, S. K., &
995 Knutti, R. (2014). Uncertainties in CMIP5 climate projections due to carbon cycle
996 feedbacks. *Journal of Climate*, 27(2), 511-526. <https://doi.org/10.1175/JCLI-D-12-00579.1>
- 997 Geil, K. L., Serra, Y. L., & Zeng, X. (2013). Assessment of CMIP5 model simulations of the
998 North American monsoon system. *Journal of Climate*, 26(22), 8787-8801.
999 <https://doi.org/10.1175/JCLI-D-13-00044.1>
- 1000 Gherardi, L. A., & Sala, O. E. (2015). Enhanced precipitation variability decreases grass-and
1001 increases shrub-productivity. *Proceedings of the National Academy of Sciences*, 112(41),
1002 12735-12740. <https://doi.org/10.1073/pnas.1506433112>
- 1003 Goberna, M., Pascual, J. A., Garcia, C., & Sánchez, J. (2007). Do plant clumps constitute
1004 microbial hotspots in semiarid Mediterranean patchy landscapes?. *Soil Biology and*
1005 *Biochemistry*, 39(5), 1047-1054. <https://doi.org/10.1016/j.soilbio.2006.11.015>
- 1006 Gomez-Casanovas, N., Matamala, R., Cook, D. R., & Gonzalez-Meler, M. A. (2012). Net
1007 ecosystem exchange modifies the relationship between the autotrophic and heterotrophic
1008 components of soil respiration with abiotic factors in prairie grasslands. *Global Change*
1009 *Biology*, 18(8), 2532-2545. <https://doi.org/10.1111/j.1365-2486.2012.02721.x>
- 1010 Goyal, R. K. (2004). Sensitivity of evapotranspiration to global warming: a case study of arid
1011 zone of Rajasthan (India). *Agricultural Water Management*, 69(1), 1-11.
1012 <https://doi.org/10.1016/j.agwat.2004.03.014>
- 1013

- 1014 Grecu, M., & Krajewski, W. F. (2000). A large-sample investigation of statistical procedures for
1015 radar-based short-term quantitative precipitation forecasting. *Journal of*
1016 *Hydrology*, 239(1), 69-84. [https://doi.org/10.1016/S0022-1694\(00\)00360-7](https://doi.org/10.1016/S0022-1694(00)00360-7)
- 1017 Gu, L., Falge, E. M., Boden, T., Baldocchi, D. D., Black, T. A., Saleska, S. R., ... & Xu, L.
1018 (2005). Objective threshold determination for nighttime eddy flux filtering. *Agricultural*
1019 *and Forest Meteorology*, 128(3), 179-197.
1020 <https://doi.org/10.1016/j.agrformet.2004.11.006>
- 1021 Gutmann, E., Pruitt, T., Clark, M. P., Brekke, L., Arnold, J. R., Raff, D. A., & Rasmussen, R. M.
1022 (2014). An intercomparison of statistical downscaling methods used for water resource
1023 assessments in the United States. *Water Resources Research*, 50(9), 7167-7186.
1024 <https://doi.org/10.1002/2014WR015559>
- 1025 Hamerlynck, E., & Knapp, A. K. (1996). Photosynthetic and stomatal responses to high
1026 temperature and light in two oaks at the western limit of their range. *Tree*
1027 *Physiology*, 16(6), 557-565. <https://doi.org/10.1093/treephys/16.6.557>
- 1028 Hamerlynck, E. P., Huxman, T. E., Loik, M. E., & Smith, S. D. (2000). Effects of extreme high
1029 temperature, drought and elevated CO₂ on photosynthesis of the Mojave Desert
1030 evergreen shrub, *Larrea tridentata*. *Plant Ecology*, 148(2), 183-193.
- 1031 Harper, C. W., Blair, J. M., Fay, P. A., Knapp, A. K., & Carlisle, J. D. (2005). Increased rainfall
1032 variability and reduced rainfall amount decreases soil CO₂ flux in a grassland
1033 ecosystem. *Global Change Biology*, 11(2), 322-334. [https://doi.org/10.1111/j.1365-](https://doi.org/10.1111/j.1365-2486.2005.00899.x)
1034 [2486.2005.00899.x](https://doi.org/10.1111/j.1365-2486.2005.00899.x)
- 1035 Hawkins, G. A., Vivoni, E. R., Robles-Morua, A., Mascaró, G., Rivera, E., & Dominguez, F.
1036 (2015). A climate change projection for summer hydrologic conditions in a semiarid
1037 watershed of central Arizona. *Journal of Arid Environments*, 118, 9-20.
1038 <https://doi.org/10.1016/j.jaridenv.2015.02.022>
- 1039 Heisler-White, J. L., Knapp, A. K., & Kelly, E. F. (2008). Increasing precipitation event size
1040 increases aboveground net primary productivity in a semi-arid
1041 grassland. *Oecologia*, 158(1), 129-140. <https://doi.org/10.1007/s00442-008-1116-9>
- 1042 Hewitson, B. C., Daron, J., Crane, R. G., Zermoglio, M. F., & Jack, C. (2014). Interrogating
1043 empirical-statistical downscaling. *Climatic Change*, 122(4), 539-554.
1044 <https://doi.org/10.1007/s10584-013-1021-z>
- 1045 Huntzinger, D. N., Post, W. M., Wei, Y., Michalak, A. M., West, T. O., Jacobson, A. R., ... &
1046 Hoffman, F. M. (2012). North American Carbon Program (NACP) regional interim
1047 synthesis: Terrestrial biospheric model intercomparison. *Ecological Modelling*, 232, 144-
1048 157. <https://doi.org/10.1016/j.ecolmodel.2012.02.004>
- 1049 Huxman, T. E., Snyder, K. A., Tissue, D., Leffler, A. J., Ogle, K., Pockman, W. T., ... &
1050 Schwinning, S. (2004). Precipitation pulses and carbon fluxes in semiarid and arid
1051 ecosystems. *Oecologia*, 141(2), 254-268. <https://doi.org/10.1007/s00442-004-1682-4>
- 1052 INEGI (2010). Conjunto Nacional de Uso de Suelo y Vegetación a escala 1:250,000, DGG-
1053 INEGI, México. Serie IV.
- 1054 IPCC (2013). Climate Change 2013: The Physical Science Basis. Contribution of Working
1055 Group I to the Fifth Assessment Report of the Intergovernmental Panel on Climate
1056 Change [Stocker, T.F., D. Qin, G.-K. Plattner, M. Tignor, S.K. Allen, J. Boschung, A.
1057 Nauels, Y. Xia, V. Bex and P.M. Midgley (eds.)]. Cambridge University Press,
1058 Cambridge, United Kingdom and New York, NY, USA, 1535 pp,
1059 [doi:10.1017/CBO9781107415324](https://doi.org/10.1017/CBO9781107415324).

- 1060 Ivanov, V. Y., Bras, R. L., & Vivoni, E. R. (2008a). Vegetation-hydrology dynamics in complex
1061 terrain of semiarid areas: 1. A mechanistic approach to modeling dynamic
1062 feedbacks. *Water Resources Research*, *44*(3). W03429,
1063 <https://doi.org/10.1029/2006WR005588>.
- 1064 Ivanov, V. Y., Bras, R. L., & Vivoni, E. R. (2008b). Vegetation-hydrology dynamics in complex
1065 terrain of semiarid areas: 1. A mechanistic approach to modeling dynamic
1066 feedbacks. *Water Resources Research*, *44*(3). W03430,
1067 <https://doi.org/10.1029/2006WR005595>.
- 1068 Jackson, R. B., Canadell, J., Ehleringer, J. R., Mooney, H. A., Sala, O. E., & Schulze, E. D.
1069 (1996). A global analysis of root distributions for terrestrial biomes. *Oecologia*, *108*(3),
1070 389-411. <https://doi.org/10.1007/BF00333714>
- 1071 Janssens, I. A., Lankreijer, H., Matteucci, G., Kowalski, A. S., Buchmann, N., Epron, D., ... &
1072 Montagnani, L. (2001). Productivity overshadows temperature in determining soil and
1073 ecosystem respiration across European forests. *Global Change Biology*, *7*(3), 269-278.
1074 <https://doi.org/10.1046/j.1365-2486.2001.00412.x>
- 1075 Jenerette, G. D., Scott, R. L., & Huete, A. R. (2010). Functional differences between summer
1076 and winter season rain assessed with MODIS-derived phenology in a semi-arid
1077 region. *Journal of Vegetation Science*, *21*(1), 16-30. <https://doi.org/10.1111/j.1654-1103.2009.01118.x>
- 1079 Kattge, J., & Knorr, W. (2007). Temperature acclimation in a biochemical model of
1080 photosynthesis: a reanalysis of data from 36 species. *Plant, Cell & Environment*, *30*(9),
1081 1176-1190. <https://doi.org/10.1111/j.1365-3040.2007.01690.x>
- 1082 Kauwe, M. G., Medlyn, B. E., Zaehle, S., Walker, A. P., Dietze, M. C., Hickler, T., ... & Smith,
1083 B. (2013). Forest water use and water use efficiency at elevated CO₂: a model-data
1084 intercomparison at two contrasting temperate forest FACE sites. *Global Change
1085 Biology*, *19*(6), 1759-1779. <http://dx.doi.org/10.1111/gcb.12164>
- 1086 Keenan, T. F., Baker, I., Barr, A., Ciais, P., Davis, K., Dietze, M., ... & Hufkens, K. (2012).
1087 Terrestrial biosphere model performance for inter-annual variability of land-atmosphere
1088 CO₂ exchange. *Global Change Biology*, *18*(6), 1971-1987.
1089 <http://dx.doi.org/10.1111/j.1365-2486.2012.02678.x>
- 1090 Kunkel, K.E. (2016) Update to data originally published in: Kunkel, K.E., D.R. Easterling, K.
1091 Hubbard, and K. Redmond. 2004. Temporal variations in frost-free season in the United
1092 States: 1895–2000. *Geophysical Research Letters*, *31*, L03201,
1093 doi:10.1029/2003GL018624.
- 1094 Lavee, H., Imeson, A. C., & Sarah, P. (1998). The impact of climate change on geomorphology
1095 and desertification along a mediterranean-arid transect. *Land Degradation &
1096 Development*, *9*(5), 407-422. [https://doi.org/10.1002/\(SICI\)1099-145X\(199809/10\)9:5<407::AID-LDR302>3.0.CO;2-6](https://doi.org/10.1002/(SICI)1099-145X(199809/10)9:5<407::AID-LDR302>3.0.CO;2-6)
- 1098 Leakey, A. D., Ainsworth, E. A., Bernacchi, C. J., Rogers, A., Long, S. P., & Ort, D. R. (2009).
1099 Elevated CO₂ effects on plant carbon, nitrogen, and water relations: six important lessons
1100 from FACE. *Journal of Experimental Botany*, *60*(10), 2859-2876.
1101 <https://doi.org/10.1093/jxb/erp096>
- 1102 Lee, J. Y., & Wang, B. (2014). Future change of global monsoon in the CMIP5. *Climate
1103 Dynamics*, *42*(1-2), 101-119. <https://doi.org/10.1007/s00382-012-1564-0>

- 1104 Legates, D. R., & McCabe, G. J. (1999). Evaluating the use of “goodness-of-fit” measures in
1105 hydrologic and hydroclimatic model validation. *Water Resources Research*, 35(1), 233-
1106 241. <https://doi.org/10.1029/1998WR900018>
- 1107 Lenton, T. M., & Huntingford, C. (2003). Global terrestrial carbon storage and uncertainties in
1108 its temperature sensitivity examined with a simple model. *Global Change Biology*, 9(10),
1109 1333-1352. <https://doi.org/10.1046/j.1365-2486.2003.00674.x>
- 1110 Li, T., Grant, R. F., & Flanagan, L. B. (2004). Climate impact on net ecosystem productivity of a
1111 semi-arid natural grassland: modeling and measurement. *Agricultural and Forest*
1112 *Meteorology*, 126(1), 99-116. <https://doi.org/10.1016/j.agrformet.2004.06.005>
- 1113 Liu, W., Zhang, Z. H. E., & Wan, S. (2009). Predominant role of water in regulating soil and
1114 microbial respiration and their responses to climate change in a semiarid
1115 grassland. *Global Change Biology*, 15(1), 184-195. <https://doi.org/10.1111/j.1365-2486.2008.01728.x>
- 1116
- 1117 Loescher, H. W., Oberbauer, S. F., Gholz, H. L., & Clark, D. B. (2003). Environmental controls
1118 on net ecosystem-level carbon exchange and productivity in a Central American tropical
1119 wet forest. *Global Change Biology*, 9(3), 396-412. <https://doi.org/10.1046/j.1365-2486.2003.00599.x>
- 1120
- 1121 Lu, X., Wang, L., & McCabe, M. F. (2016). Elevated CO₂ as a driver of global dryland
1122 greening. *Scientific Reports*, 6, 20716. <https://doi.org/10.1038/srep20716>
- 1123 Luo, Y., Gerten, D., Le Maire, G., Parton, W. J., Weng, E., Zhou, X., ... & Dukes, J. S. (2008).
1124 Modeled interactive effects of precipitation, temperature, and [CO₂] on ecosystem carbon
1125 and water dynamics in different climatic zones. *Global Change Biology*, 14(9), 1986-
1126 1999. <https://doi.org/10.1111/j.1365-2486.2008.01629.x>
- 1127 Luo, Y., Wan, S., Hui, D., & Wallace, L. L. (2001). Acclimatization of soil respiration to
1128 warming in a tall grass prairie. *Nature*, 413(6856), 622-625.
1129 <https://doi.org/10.1038/35098065>
- 1130 Lloyd, J., & Taylor, J. A. (1994). On the temperature dependence of soil respiration. *Functional*
1131 *Ecology*, 8(3), 315-323. <https://doi.org/10.2307/2389824>
- 1132 Maloney, E. D., Camargo, S. J., Chang, E., Colle, B., Fu, R., Geil, K. L., ... & Kinter, J. (2014).
1133 North American climate in CMIP5 experiments: Part III: Assessment of twenty-first-
1134 century projections. *Journal of Climate*, 27(6), 2230-2270. <https://doi.org/10.1175/JCLI-D-13-00273.1>
- 1135
- 1136 Manzoni, S., Porporato, A., D'Odorico, P., Laio, F., & Rodriguez-Iturbe, I. (2004). Soil nutrient
1137 cycles as a nonlinear dynamical system. *Nonlinear Processes in Geophysics*, 11(5/6),
1138 589-598.
- 1139 Maraun, D. (2013). Bias correction, quantile mapping, and downscaling: revisiting the inflation
1140 issue. *Journal of Climate*, 26(6), 2137-2143. <https://doi.org/10.1175/JCLI-D-12-00821.1>
- 1141 Martínez-Yrizar, A., Núñez, S., & Burquez, A. (2007). Leaf litter decomposition in a southern
1142 Sonoran Desert ecosystem, northwestern Mexico: Effects of habitat and litter
1143 quality. *Acta Oecologica*, 32(3), 291-300. <https://doi.org/10.1016/j.actao.2007.05.010>
- 1144 Martínez-Yrizar, A., Núñez, S., Miranda, H., & Búrquez, A. (1999). Temporal and spatial
1145 variation of litter production in Sonoran Desert communities. *Plant Ecology*, 145(1), 37-
1146 48. <https://doi.org/10.1023/A:1009896201047>
- 1147 Maseyk, K., Hemming, D., Angert, A., Leavitt, S. W., & Yakir, D. (2011). Increase in water-use
1148 efficiency and underlying processes in pine forests across a precipitation gradient in the

1149 dry Mediterranean region over the past 30 years. *Oecologia*, 167(2), 573-585.
1150 <https://doi.org/10.1007/s00442-011-2010-4>

1151 Massman, W. J., & Lee, X. (2002). Eddy covariance flux corrections and uncertainties in long-
1152 term studies of carbon and energy exchanges. *Agricultural and Forest*
1153 *Meteorology*, 113(1), 121-144. [https://doi.org/10.1016/S0168-1923\(02\)00105-3](https://doi.org/10.1016/S0168-1923(02)00105-3)

1154 McCulley, R. L., Archer, S. R., Boutton, T. W., Hons, F. M., & Zuberer, D. A. (2004). Soil
1155 respiration and nutrient cycling in wooded communities developing in
1156 grassland. *Ecology*, 85(10), 2804-2817. <https://doi.org/10.1890/03-0645>

1157 Méndez-Barroso, L. A., Vivoni, E. R., Watts, C. J., & Rodríguez, J. C. (2009). Seasonal and
1158 interannual relations between precipitation, surface soil moisture and vegetation
1159 dynamics in the North American monsoon region. *Journal of Hydrology*, 377(1), 59-70.
1160 <https://doi.org/10.1016/j.jhydrol.2009.08.009>

1161 Méndez-Barroso, L. A., Vivoni, E. R., Robles-Morua, A., Mascaro, G., Yépez, E. A., Rodríguez,
1162 J. C., ... & Saíz-Hernández, J. A. (2014). A modeling approach reveals differences in
1163 evapotranspiration and its partitioning in two semiarid ecosystems in Northwest
1164 Mexico. *Water Resources Research*, 50(4), 3229-3252.
1165 <https://doi.org/10.1002/2013WR014838>

1166 Miranda, J. D. D., Armas, C., Padilla, F. M., & Pugnaire, F. I. (2011). Climatic change and
1167 rainfall patterns: effects on semi-arid plant communities of the Iberian Southeast. *Journal*
1168 *of Arid Environments*, 75(12), 1302-1309. <https://doi.org/10.1016/j.jaridenv.2011.04.022>

1169 Mitchell, K. E., Lohmann, D., Houser, P. R., Wood, E. F., Schaake, J. C., Robock, A., ... &
1170 Higgins, R. W. (2004). The multi-institution North American Land Data Assimilation
1171 System (NLDAS): Utilizing multiple GCIP products and partners in a continental
1172 distributed hydrological modeling system. *Journal of Geophysical Research:*
1173 *Atmospheres*, 109(D7). <https://doi.org/10.1029/2003JD003823>

1174 Morgan, J. A., Mosier, A. R., Milchunas, D. G., LeCain, D. R., Nelson, J. A., & Parton, W. J.
1175 (2004). CO₂ enhances productivity of the shortgrass steppe, alters species composition,
1176 and reduces forage digestibility. *Ecological Applications*, 14, 208-219.

1177 Morgan, J. A., LeCain, D. R., Pendall, E., Blumenthal, D. M., Kimball, B. A., Carrillo, Y., ... &
1178 West, M. (2011). C₄ grasses prosper as carbon dioxide eliminates desiccation in warmed
1179 semi-arid grassland. *Nature*, 476(7359), 202-205. <http://dx.doi.org/10.1038/nature10274>

1180 Moritz, C., & Agudo, R. (2013). The future of species under climate change: resilience or
1181 decline?. *Science*, 341(6145), 504-508. <https://doi.org/10.1126/science.1237190>

1182 Mowll, W., Blumenthal, D. M., Cherwin, K., Smith, A., Symstad, A. J., Vermeire, L. T., ... &
1183 Knapp, A. K. (2015). Climatic controls of aboveground net primary production in semi-
1184 arid grasslands along a latitudinal gradient portend low sensitivity to
1185 warming. *Oecologia*, 177(4), 959-969. <https://doi.org/10.1007/s0044>

1186 Mueller, K. E., Blumenthal, D. M., Pendall, E., Carrillo, Y., Dijkstra, F. A., Williams, D. G., ...
1187 & Morgan, J. A. (2016). Impacts of warming and elevated CO₂ on a semi-arid grassland
1188 are non-additive, shift with precipitation, and reverse over time. *Ecology Letters*, 19(8),
1189 956-966. <https://doi.org/10.1111/ele.12634>

1190 Nagol, J. R., Vermote, E. F., & Prince, S. D. (2009). Effects of atmospheric variation on
1191 AVHRR NDVI data. *Remote Sensing of Environment*, 113(2), 392-397.
1192 <https://doi.org/10.1016/j.rse.2008.10.007>

1193 Nayak, R. K., Patel, N. R., & Dadhwal, V. K. (2015). Spatio-temporal variability of net
1194 ecosystem productivity over India and its relationship to climatic

1195 variables. *Environmental Earth Sciences*, 74(2), 1743-1753.
1196 <https://doi.org/10.1007/s12665-015-4182-4>
1197 Newingham, B. A., Vanier, C. H., Charlet, T. N., Ogle, K., Smith, S. D., & Nowak, R. S. (2013).
1198 No cumulative effect of 10 years of elevated [CO₂] on perennial plant biomass
1199 components in the Mojave Desert. *Global Change Biology*, 19(7), 2168-2181.
1200 <https://doi.org/10.1111/gcb.12177>
1201 Novick, K. A., Ficklin, D. L., Stoy, P. C., Williams, C. A., Bohrer, G., Oishi, A. C., Papuga, S.
1202 A., Blanken, P. D., Noormets, A., Sulman, B. N., Scott, R. L., Wang, L., & Phillips, R. P.
1203 (2016). The increasing importance of atmospheric demand for ecosystem water and
1204 carbon fluxes. *Nature Climate Change*, 6(11), 1023-1027.
1205 <http://dx.doi.org/10.1038/nclimate3114>
1206 Núñez, S., Martínez-Yrizar, A., Búrquez, A., & García-Oliva, F. (2001). Carbon mineralization
1207 in the southern Sonoran Desert. *Acta Oecologica*, 22(5), 269-276.
1208 [https://doi.org/10.1016/S1146-609X\(01\)01122-5](https://doi.org/10.1016/S1146-609X(01)01122-5)
1209 Ogle, K., & Reynolds, J. F. (2002). Desert dogma revisited: coupling of stomatal conductance
1210 and photosynthesis in the desert shrub, *Larrea tridentata*. *Plant, Cell &*
1211 *Environment*, 25(7), 909-921. <https://doi.org/10.1046/j.1365-3040.2002.00876.x>
1212 ORNL DAAC. 2008. MODIS Collection 5 Land Products Global Subsetting and Visualization
1213 Tool. ORNL DAAC, Oak Ridge, Tennessee, USA. Accessed January 18,
1214 2017. <http://dx.doi.org/10.3334/ORNLDAAC/1241>
1215 Pachauri, R. K., Allen, M. R., Barros, V. R., Broome, J., Cramer, W., Christ, R., ... & Dubash, N.
1216 K. (2014). *Climate change 2014: synthesis report. Contribution of Working Groups I, II*
1217 *and III to the fifth assessment report of the Intergovernmental Panel on Climate*
1218 *Change* (p. 151). IPCC.
1219 Parolari, A. J., & Porporato, A. (2016). Forest soil carbon and nitrogen cycles under biomass
1220 harvest: stability, transient response, and feedback. *Ecological Modelling*, 329, 64-76.
1221 <https://doi.org/10.1016/j.ecolmodel.2016.03.003>
1222 Pavón, N. P., Briones, O., & Flores-Rivas, J. (2005). Litterfall production and nitrogen content in
1223 an intertropical semi-arid Mexican scrub. *Journal of Arid Environments*, 60(1), 1-13.
1224 <https://doi.org/10.1016/j.jaridenv.2004.03.004>
1225 Perez-Ruiz, E. R., Garatuza-Payan, J., Watts, C. J., Rodriguez, J. C., Yezpe, E. A., & Scott, R. L.
1226 (2010). Carbon dioxide and water vapour exchange in a tropical dry forest as influenced
1227 by the North American Monsoon System (NAMS). *Journal of Arid Environments*, 74(5),
1228 556-563. <https://doi.org/10.1016/j.jaridenv.2009.09.029>
1229 Plaut, J. A., Yezpe, E. A., Hill, J., Pangle, R., Sperry, J. S., Pockman, W. T., & McDowell, N. G.
1230 (2012). Hydraulic limits preceding mortality in a piñon-juniper woodland under
1231 experimental drought. *Plant, Cell & Environment*, 35(9), 1601-1617.
1232 <https://doi.org/10.1111/j.1365-3040.2012.02512.x>
1233 Ponce-Campos, G. E., Moran, M. S., Huete, A., Zhang, Y., Bresloff, C., Huxman, T. E., ... &
1234 Scalley, T. H. (2013). Ecosystem resilience despite large-scale altered hydroclimatic
1235 conditions. *Nature*, 494(7437), 349-352. <https://doi.org/10.1038/nature11836>
1236 Porporato, A., D'odorico, P., Laio, F., & Rodriguez-Iturbe, I. (2003). Hydrologic controls on soil
1237 carbon and nitrogen cycles. I. Modeling scheme. *Advances in Water Resources*, 26(1),
1238 45-58. [https://doi.org/10.1016/S0309-1708\(02\)00094-5](https://doi.org/10.1016/S0309-1708(02)00094-5)

- 1239 Poulter, B., Frank, D., Ciais, P., Myneni, R. B., Andela, N., Bi, J., ... & Running, S. W. (2014).
1240 Contribution of semi-arid ecosystems to interannual variability of the global carbon
1241 cycle. *Nature*, *509*(7502), 600-603. <https://doi.org/10.1038/nature13376>
1242 Rawls, W. J., Brakensiek, D. L., & Saxton, K. E. (1982). Estimation of soil water
1243 properties. *Transactions of the ASAE*, *25*(5), 1316-1320.
1244 <https://doi.org/10.13031/2013.33720>
1245 Reichstein, M., Falge, E., Baldocchi, D., Papale, D., Aubinet, M., Berbigier, P., ... & Grünwald,
1246 T. (2005). On the separation of net ecosystem exchange into assimilation and ecosystem
1247 respiration: review and improved algorithm. *Global Change Biology*, *11*(9), 1424-1439.
1248 <https://doi.org/10.1111/j.1365-2486.2005.001002.x>
1249 Reichstein, M., Rey, A., Freibauer, A., Tenhunen, J., Valentini, R., Banza, J., ... & Joffre, R.
1250 (2003). Modeling temporal and large-scale spatial variability of soil respiration from soil
1251 water availability, temperature and vegetation productivity indices. *Global*
1252 *Biogeochemical Cycles*, *17*, 1104. <https://doi.org/10.1029/2003GB002035>
1253 Robertson, T. R., Bell, C. W., Zak, J. C., & Tissue, D. T. (2009). Precipitation timing and
1254 magnitude differentially affect aboveground annual net primary productivity in three
1255 perennial species in a Chihuahuan Desert grassland. *New Phytologist*, *181*(1), 230-242.
1256 <https://doi.org/10.1111/j.1469-8137.2008.02643.x>
1257 Robles-Morua, A., Vivoni, E. R., & Mayer, A. S. (2012). Distributed hydrologic modeling in
1258 northwest Mexico reveals the links between runoff mechanisms and
1259 evapotranspiration. *Journal of Hydrometeorology*, *13*(3), 785-807.
1260 <https://doi.org/10.1175/JHM-D-11-0112.1>
1261 Robles-Morua, A., Che, D., Mayer, A. S., & Vivoni, E. R. (2015). Hydrological assessment of
1262 proposed reservoirs in the Sonora River Basin, Mexico, under historical and future
1263 climate scenarios. *Hydrological Sciences Journal*, *60*(1), 50-66.
1264 <https://doi.org/10.1080/02626667.2013.878462>
1265 Porporato, A., D'odorico, P., Laio, F., Ridolfi, L., & Rodriguez-Iturbe, I. (2003). Ecohydrology
1266 of water-controlled ecosystems. *Advances in Water Resources*, *25*(8), 1335-1348.
1267 [https://doi.org/10.1016/S0309-1708\(02\)00058-1](https://doi.org/10.1016/S0309-1708(02)00058-1)
1268 Rohr, T., Manzoni, S., Feng, X., Menezes, R. S., & Porporato, A. (2013). Effect of rainfall
1269 seasonality on carbon storage in tropical dry ecosystems. *Journal of Geophysical*
1270 *Research: Biogeosciences*, *118*(3), 1156-1167. <https://doi.org/10.1002/jgrg.20091>
1271 Ross, I., Misson, L., Rambal, S., Arneth, A., Scott, R. L., Carrara, A., ... & Genesio, L. (2012).
1272 How do variations in the temporal distribution of rainfall events affect ecosystem fluxes
1273 in seasonally water-limited Northern Hemisphere shrublands and
1274 forests. *Biogeosciences*, *9*, 1007-1024. <http://dx.doi.org/10.5194/bg-9-1007-2012>
1275 Ryan, M. G. (1991). Effects of climate change on plant respiration. *Ecological*
1276 *Applications*, *1*(2), 157-167. <http://doi.org/10.2307/1941808>
1277 Sacks, W. J., Schimel, D. S., & Monson, R. K. (2007). Coupling between carbon cycling and
1278 climate in a high-elevation, subalpine forest: a model-data fusion
1279 analysis. *Oecologia*, *151*(1), 54-68. <https://doi.org/10.1007/s00442-006-0565-2>
1280 Sage, R. F., & Kubien, D. S. (2007). The temperature response of C3 and C4
1281 photosynthesis. *Plant, Cell & Environment*, *30*(9), 1086-1106.
1282 <https://doi.org/10.1111/j.1365-3040.2007.01682.x>

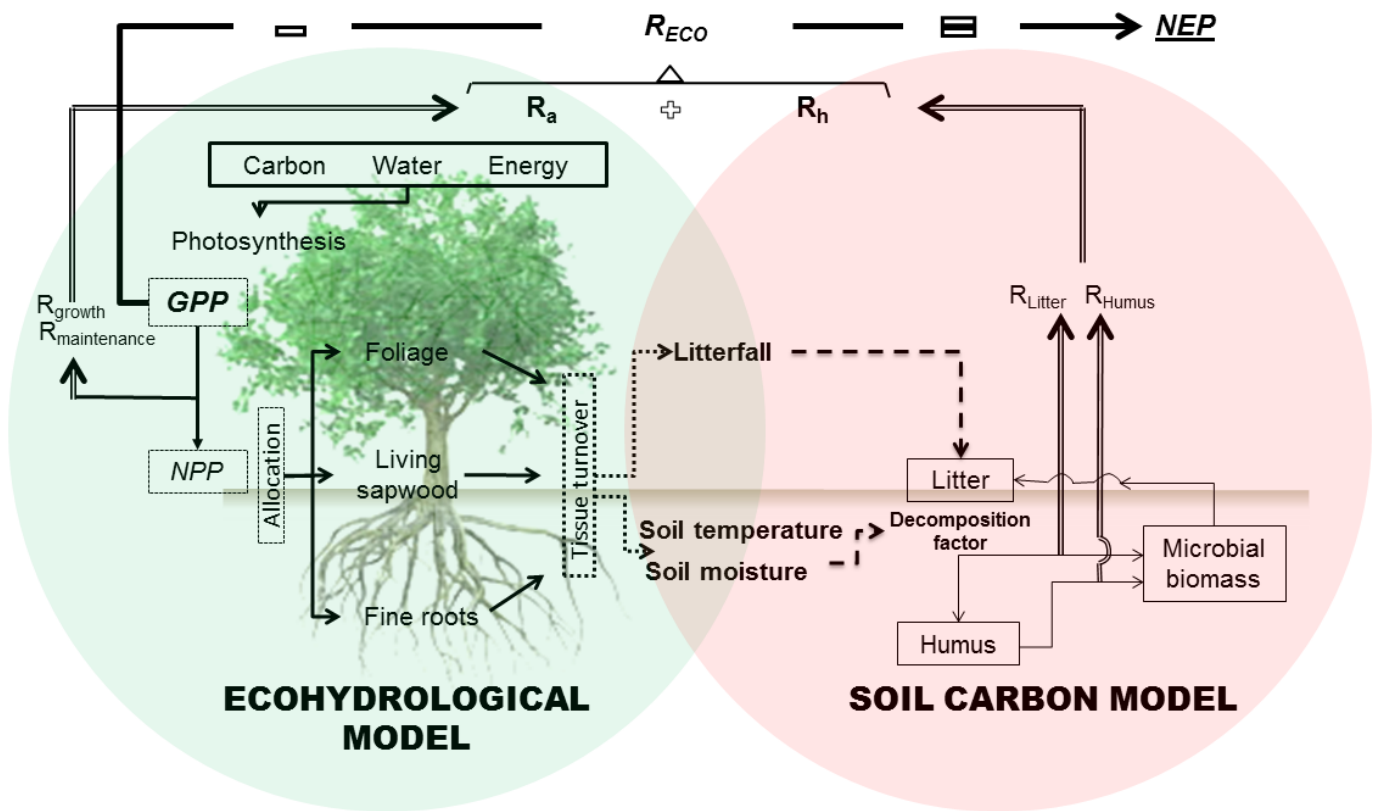
- 1283 Sage, R. F., Sharkey, T. D., & Seemann, J. R. (1989). Acclimation of photosynthesis to elevated
1284 CO₂ in five C₃ species. *Plant Physiology*, 89(2), 590-596.
1285 <https://doi.org/10.1104/pp.89.2.590>
- 1286 Salvucci, M. E., & Crafts-Brandner, S. J. (2004). Relationship between the heat tolerance of
1287 photosynthesis and the thermal stability of Rubisco activase in plants from contrasting
1288 thermal environments. *Plant Physiology*, 134(4), 1460-1470.
1289 <https://doi.org/10.1104/pp.103.038323>
- 1290 Seneviratne, S. I., Corti, T., Davin, E. L., Hirschi, M., Jaeger, E. B., Lehner, I., ... & Teuling, A.
1291 J. (2010). Investigating soil moisture–climate interactions in a changing climate: A
1292 review. *Earth-Science Reviews*, 99(3), 125-161.
1293 <https://doi.org/10.1016/j.earscirev.2010.02.004>
- 1294 Scott, R. L., Biederman, J. A., Hamerlynck, E. P., & Barron-Gafford, G. A. (2015). The carbon
1295 balance pivot point of southwestern US semiarid ecosystems: Insights from the 21st
1296 century drought. *Journal of Geophysical Research: Biogeosciences*, 120(12), 2612-2624.
1297 <https://doi.org/10.1002/2015JG003181>
- 1298 Scott, R. L., Edwards, E. A., Shuttleworth, W. J., Huxman, T. E., Watts, C., & Goodrich, D. C.
1299 (2004). Interannual and seasonal variation in fluxes of water and carbon dioxide from a
1300 riparian woodland ecosystem. *Agricultural and Forest Meteorology*, 122(1), 65-84.
1301 <https://doi.org/10.1016/j.agrformet.2003.09.001>
- 1302 Scott, R. L., Hamerlynck, E. P., Jenerette, G. D., Moran, M. S., & Barron-Gafford, G. A. (2010).
1303 Carbon dioxide exchange in a semidesert grassland through drought-induced vegetation
1304 change. *Journal of Geophysical Research: Biogeosciences*, 115, G03026,
1305 <https://doi.org/10.1029/2010JG001348>
- 1306 Scott, R. L., Jenerette, G. D., Potts, D. L., & Huxman, T. E. (2009). Effects of seasonal drought
1307 on net carbon dioxide exchange from a woody-plant-encroached semiarid
1308 grassland. *Journal of Geophysical Research: Biogeosciences*, 114, G04004,
1309 <https://doi.org/doi:10.1029/2008JG000900>
- 1310 Schwinning, S., & Ehleringer, J. R. (2001). Water use trade-offs and optimal adaptations to
1311 pulse-driven arid ecosystems. *Journal of Ecology*, 89(3), 464-480.
1312 <https://doi.org/10.1046/j.1365-2745.2001.00576.x>
- 1313 Seager, R., Ting, M., Held, I., Kushnir, Y., Lu, J., Vecchi, G., ... & Li, C. (2007). Model
1314 projections of an imminent transition to a more arid climate in southwestern North
1315 America. *Science*, 316(5828), 1181-1184. <https://doi.org/10.1126/science.1139601>
- 1316 Serrat-Capdevila, A., Scott, R. L., Shuttleworth, W. J., & Valdés, J. B. (2011). Estimating
1317 evapotranspiration under warmer climates: Insights from a semi-arid riparian
1318 system. *Journal of Hydrology*, 399(1), 1-11.
1319 <https://doi.org/10.1016/j.jhydrol.2010.12.021>
- 1320 Shi, Z., Thomey, M. L., Mowll, W., Litvak, M., Brunsell, N. A., Collins, S. L., ... & Luo, Y.
1321 (2013). Differential effects of extreme drought on production and respiration: synthesis
1322 and modeling analysis. *Biogeosciences Discussions*, 10(10), 16043-16074.
1323 <https://doi.org/10.5194/bg-11-621-2014>, 2014
- 1324 Sivandran, G., & Bras, R. L. (2012) Identifying the optimal spatially and temporally invariant
1325 root distributions for a semiarid environment. *Water Resources Research*, 48, W12525.
1326 <http://dx.doi.org/10.1029/2012WR012055>.

- 1327 Slot, M., & Kitajima, K. (2015). General patterns of acclimation of leaf respiration to elevated
1328 temperatures across biomes and plant types. *Oecologia*, *177*(3), 885-900.
1329 <https://doi.org/10.1007/s00442-014-3159-4>
- 1330 Smith, S. D., Huxman, T. E., Zitzer, S. F., Charlet, T. N., Housman, D. C., Coleman, J. S., ... &
1331 Nowak, R. S. (2000). Elevated CO₂ increases productivity and invasive species success
1332 in an arid ecosystem. *Nature*, *408*(6808), 79-82. <https://doi.org/10.1038/35040544>
- 1333 Spitters, C. J. T., Toussaint, H. A. J. M., & Goudriaan, J. (1986). Separating the diffuse and
1334 direct component of global radiation and its implications for modeling canopy
1335 photosynthesis Part I. Components of incoming radiation. *Agricultural and Forest
1336 Meteorology*, *38*(1-3), 217-229. [https://doi.org/10.1016/0168-1923\(86\)90060-2](https://doi.org/10.1016/0168-1923(86)90060-2)
- 1337 Sponseller, R. A. (2007). Precipitation pulses and soil CO₂ flux in a Sonoran Desert
1338 ecosystem. *Global Change Biology*, *13*(2), 426-436. [https://doi.org/10.1111/j.1365-
2486.2006.01307.x](https://doi.org/10.1111/j.1365-
1339 2486.2006.01307.x)
- 1340 Steinweg, J. M., Plante, A. F., Conant, R. T., Paul, E. A., & Tanaka, D. L. (2008). Patterns of
1341 substrate utilization during long-term incubations at different temperatures. *Soil Biology
1342 and Biochemistry*, *40*(11), 2722-2728. <https://doi.org/10.1016/j.soilbio.2008.07.002>
- 1343 Stoy, P. C., Katul, G. G., Siqueira, M. B., Juang, J. Y., Novick, K. A., Uebelherr, J. M., & Oren,
1344 R. (2006). An evaluation of models for partitioning eddy covariance-measured net
1345 ecosystem exchange into photosynthesis and respiration. *Agricultural and Forest
1346 Meteorology*, *141*(1), 2-18. <https://doi.org/10.1016/j.agrformet.2006.09.001>
- 1347 Stoy, P. C., Richardson, A. D., Baldocchi, D. D., Katul, G. G., Stanovick, J., Mahecha, M. D., ...
1348 & Arriga, N. (2009). Biosphere-atmosphere exchange of CO₂ in relation to
1349 climate. *Biogeosciences*, *6*, 2297-2312. <https://doi.org/10.5194/bg-6-2297-2009>
- 1350 Tang, Q., Vivoni, E. R., Muñoz-Arriola, F., & Lettenmaier, D. P. (2012). Predictability of
1351 evapotranspiration patterns using remotely sensed vegetation dynamics during the North
1352 American monsoon. *Journal of Hydrometeorology*, *13*(1), 103-121.
1353 <https://doi.org/10.1175/JHM-D-11-032.1>
- 1354 Taylor, K. E., Stouffer, R. J., & Meehl, G. A. (2012). An overview of CMIP5 and the experiment
1355 design. *Bulletin of the American Meteorological Society*, *93*(4), 485-498.
1356 <https://doi.org/10.1175/BAMS-D-11-00094.1>
- 1357 Thiessen, S., Gleixner, G., Wutzler, T., & Reichstein, M. (2013). Both priming and temperature
1358 sensitivity of soil organic matter decomposition depend on microbial biomass—An
1359 incubation study. *Soil Biology and Biochemistry*, *57*, 739-748.
1360 <https://doi.org/10.1016/j.soilbio.2012.10.029>
- 1361 Thomey, M. L., Collins, S. L., Vargas, R., Johnson, J. E., Brown, R. F., Natvig, D. O., &
1362 Friggens, M. T. (2011). Effect of precipitation variability on net primary production and
1363 soil respiration in a Chihuahuan Desert grassland. *Global Change Biology*, *17*(4), 1505-
1364 1515. <https://doi.org/10.1111/j.1365-2486.2010.02363.x>
- 1365 Unger, S., Máguas, C., Pereira, J. S., David, T. S., & Werner, C. (2010). The influence of
1366 precipitation pulses on soil respiration—Assessing the “Birch effect” by stable carbon
1367 isotopes. *Soil Biology and Biochemistry*, *42*(10), 1800-1810.
1368 <https://doi.org/10.1016/j.soilbio.2010.06.019>
- 1369 Vargas, R., Sonnentag, O., Abramowitz, G., Carrara, A., Chen, J. M., Ciais, P., Correia, A.,
1370 Keenan, T. F., Kobayashi, H. & Ourcival, J.-M. (2013). Drought influences the accuracy
1371 of simulated ecosystem fluxes: a model-data meta-analysis for Mediterranean oak
1372 woodlands. *Ecosystems*, *16*, 749-764. <https://doi.org/10.1007/s10021-013-9648-1>

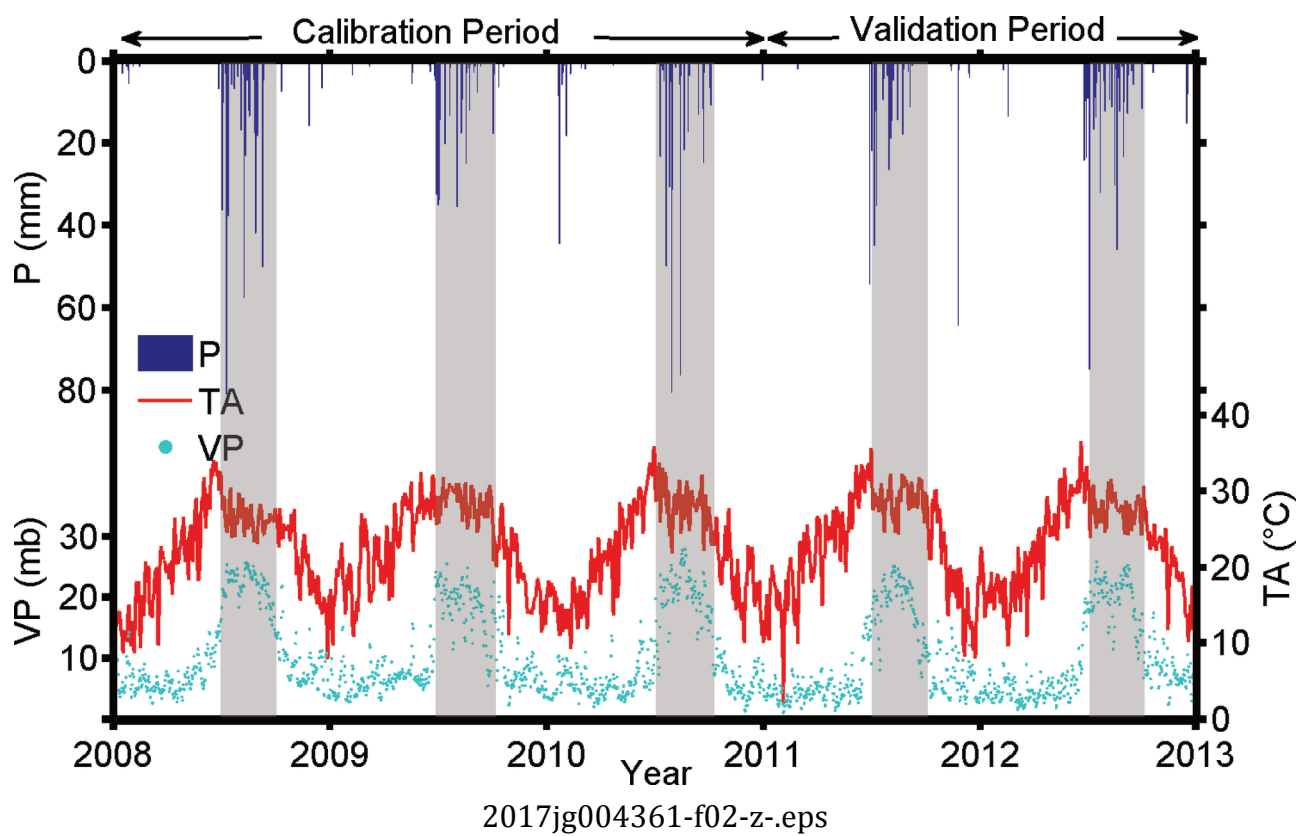
- 1373 Verduzco, V. S., Garatuza-Payán, J., Yépez, E. A., Watts, C. J., Rodríguez, J. C., Robles-Morua,
1374 A., & Vivoni, E. R. (2015). Variations of net ecosystem production due to seasonal
1375 precipitation differences in a tropical dry forest of northwest Mexico. *Journal of*
1376 *Geophysical Research: Biogeosciences*, *120*(10), 2081-2094.
1377 <https://doi.org/10.1002/2015JG003119>
- 1378 Verduzco, V. S. (2016). *Climate Variability Impacts on Net Ecosystem Production in Northwest*
1379 *Mexico*. Ph.D. Dissertation in Biotechnology, Instituto Tecnológico de Sonora, Ciudad
1380 Obregón, Sonora, México, 169 pp.
- 1381 Villarreal, S., Vargas, R., Yépez, E. A., Acosta, J. S., Castro, A., Escoto-Rodríguez, M., ... &
1382 Vivoni, E. R. (2016). Contrasting precipitation seasonality influences evapotranspiration
1383 dynamics in water-limited shrublands. *Journal of Geophysical Research:*
1384 *Biogeosciences*, *121*(2), 494-508. <https://doi.org/10.1002/2015JG003169>
- 1385 Vivoni, E. R., Ivanov, V. Y., Bras, R. L., & Entekhabi, D. (2005). On the effects of triangulated
1386 terrain resolution on distributed hydrologic model response. *Hydrological*
1387 *Processes*, *19*(11), 2101-2122. 10.1002/hyp.5671 10.1002/hyp.5671
- 1388 Vivoni, E. R., Entekhabi, D., Bras, R. L., Ivanov, V. Y., Van Horne, M. P., Grassotti, C., &
1389 Hoffman, R. N. (2006). Extending the predictability of hydrometeorological flood events
1390 using radar rainfall nowcasting. *Journal of Hydrometeorology*, *7*(4), 660-677.
1391 <https://doi.org/10.1175/JHM514.1>
- 1392 Vivoni, E. R., Moreno, H. A., Mascaro, G., Rodriguez, J. C., Watts, C. J., Garatuza-Payan, J., &
1393 Scott, R. L. (2008). Observed relation between evapotranspiration and soil moisture in
1394 the North American monsoon region. *Geophysical Research Letters*, *35*(22), L22403,
1395 <https://doi.org/10.1029/2008GL036001>.
- 1396 Vivoni, E. R., Rodríguez, J. C., & Watts, C. J. (2010). On the spatiotemporal variability of soil
1397 moisture and evapotranspiration in a mountainous basin within the North American
1398 monsoon region. *Water Resources Research*, *46*(2), W02509,
1399 <https://doi.org/10.1029/2009WR008240>.
- 1400 Vivoni, E. R., Watts, C. J., Rodríguez, J. C., Garatuza-Payan, J., Méndez-Barroso, L. A., & Saiz-
1401 Hernández, J. A. (2010). Improved land-atmosphere relations through distributed
1402 footprint sampling in a subtropical scrubland during the North American
1403 monsoon. *Journal of Arid Environments*, *74*(5), 579-584.
1404 <https://doi.org/10.1016/j.jaridenv.2009.09.031>
- 1405 Wang, D., Heckathorn, S. A., Wang, X., & Philpott, S. M. (2012). A meta-analysis of plant
1406 physiological and growth responses to temperature and elevated CO₂. *Oecologia*, *169*(1),
1407 1-13. <https://doi.org/10.1007/s00442-011-2172-0>.
- 1408 Wang, Y. P., & Leuning, R. (1998). A two-leaf model for canopy conductance, photosynthesis
1409 and partitioning of available energy I: Model description and comparison with a multi-
1410 layered model. *Agricultural and Forest Meteorology*, *91*(1), 89-111.
1411 [https://doi.org/10.1016/S0168-1923\(98\)00061-6](https://doi.org/10.1016/S0168-1923(98)00061-6)
- 1412 Watts, C. J., Scott, R. L., Garatuza-Payan, J., Rodriguez, J. C., Prueger, J. H., Kustas, W. P., &
1413 Douglas, M. (2007). Changes in vegetation condition and surface fluxes during NAME
1414 2004. *Journal of Climate*, *20*(9), 1810-1820. <https://doi.org/10.1175/JCLI4088.1>
- 1415 Webb, E. K., Pearman, G. I., & Leuning, R. (1980). Correction of flux measurements for density
1416 effects due to heat and water vapour transfer. *Quarterly Journal of the Royal*
1417 *Meteorological Society*, *106*(447), 85-100. <https://doi.org/10.1002/qj.49710644707>

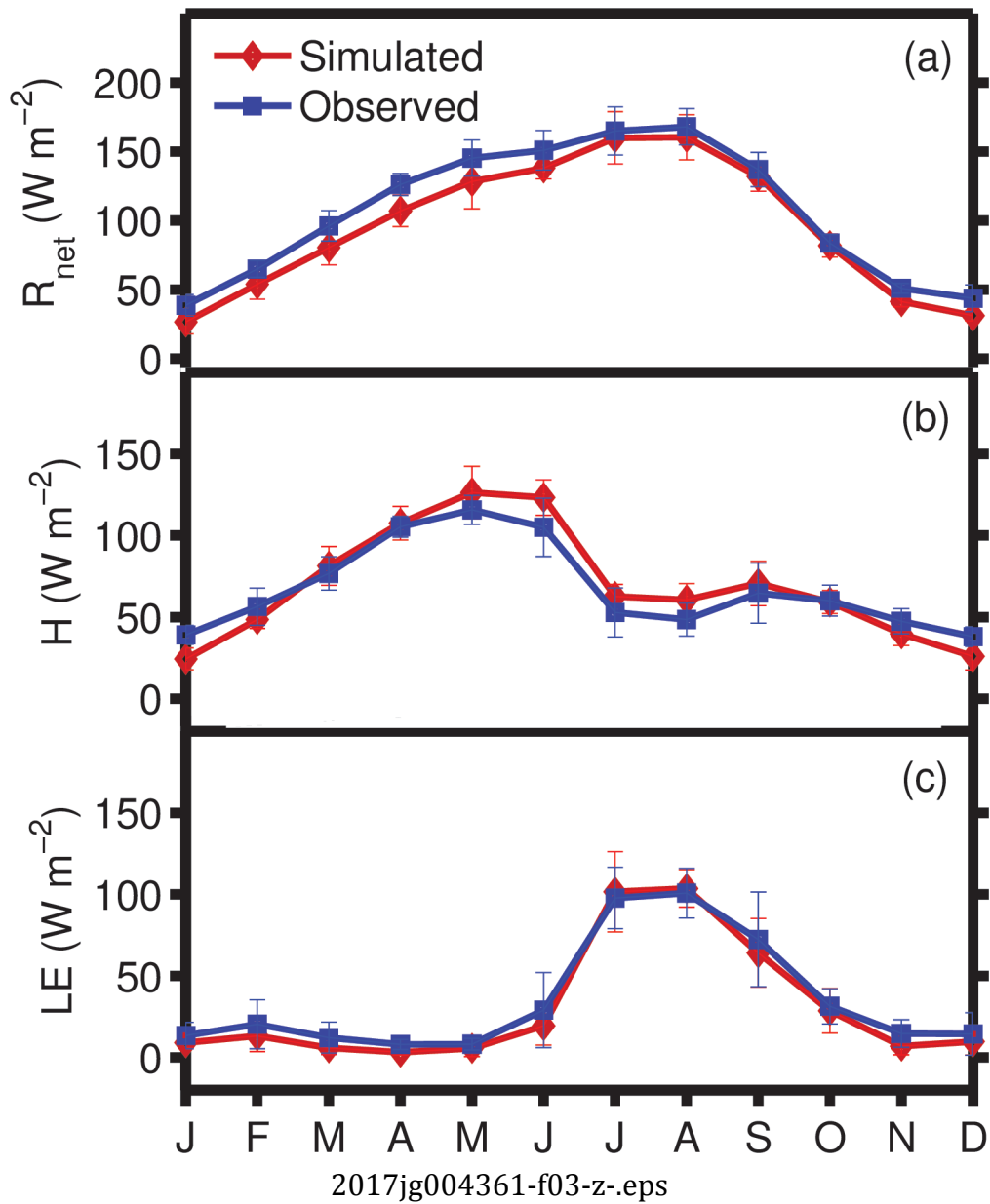
- 1418 Werk, K. S., Ehleringer, J., Forseth, I. N., & Cook, C. S. (1983). Photosynthetic characteristics of
1419 Sonoran Desert winter annuals. *Oecologia*, 59(1), 101-105.
1420 <https://doi.org/10.1007/BF00388081>
- 1421 Wilcke, R. A. I., Mendlik, T., & Gobiet, A. (2013). Multi-variable error correction of regional
1422 climate models. *Climatic Change*, 120(4), 871-887. [https://doi.org/10.1007/s10584-013-](https://doi.org/10.1007/s10584-013-0845-x)
1423 0845-x
- 1424 Wilczak, J. M., Oncley, S. P., & Stage, S. A. (2001). Sonic anemometer tilt correction
1425 algorithms. *Boundary-Layer Meteorology*, 99(1), 127-150.
1426 <https://doi.org/10.1023/A:1018966204465>
- 1427 Williams, A. P., Allen, C. D., Macalady, A. K., Griffin, D., Woodhouse, C. A., Meko, D. M., ...
1428 & Dean, J. S. (2013). Temperature as a potent driver of regional forest drought stress and
1429 tree mortality. *Nature Climate Change*, 3(3), 292-297.
1430 <https://doi.org/10.1038/nclimate1693>
- 1431 Wullschleger, S. D., Gunderson, C. A., Hanson, P. J., Wilson, K. B., & Norby, R. J. (2002).
1432 Sensitivity of stomatal and canopy conductance to elevated CO₂ concentration—
1433 interacting variables and perspectives of scale. *New Phytologist*, 153(3), 485-496.
1434 <https://doi.org/10.1046/j.0028-646X.2001.00333.x>
- 1435 Wu, J., Linden, L. V. D., Lasslop, G., Carvalhais, N., Pilegaard, K., Beier, C., & Ibrom, A.
1436 (2012). Effects of climate variability and functional changes on the interannual variation
1437 of the carbon balance in a temperate deciduous forest. *Biogeosciences*, 9(1), 13-28.
1438 <https://doi.org/10.5194/bg-9-13-2012>
- 1439 Wu, Z., Dijkstra, P., Koch, G. W., Penuelas, J., & Hungate, B. A. (2011). Responses of terrestrial
1440 ecosystems to temperature and precipitation change: a meta-analysis of experimental
1441 manipulation. *Global Change Biology*, 17(2), 927-942. [https://doi.org/10.1111/j.1365-](https://doi.org/10.1111/j.1365-2486.2010.02302.x)
1442 2486.2010.02302.x
- 1443 Xiao, J., Zhuang, Q., Law, B. E., Baldocchi, D. D., Chen, J., Richardson, A. D., ... & Oren, R.
1444 (2011). Assessing net ecosystem carbon exchange of US terrestrial ecosystems by
1445 integrating eddy covariance flux measurements and satellite observations. *Agricultural
1446 and Forest Meteorology*, 151(1), 60-69. <https://doi.org/10.1016/j.agrformet.2010.09.002>
- 1447 Xie, J., Zha, T., Jia, X., Qian, D., Wu, B., Zhang, Y., ... & Peltola, H. (2015). Irregular
1448 precipitation events in control of seasonal variations in CO₂ exchange in a cold desert-
1449 shrub ecosystem in northwest China. *Journal of Arid Environments*, 120, 33-41.
1450 <https://doi.org/10.1016/j.jaridenv.2015.04.009>
- 1451 Xu, C., McDowell, N. G., Sevanto, S., & Fisher, R. A. (2013). Our limited ability to predict
1452 vegetation dynamics under water stress. *New Phytologist*, 200(2), 298-300.
1453 <https://doi.org/10.1111/nph.12450>
- 1454 Xu, L., & Baldocchi, D. D. (2004). Seasonal variation in carbon dioxide exchange over a
1455 Mediterranean annual grassland in California. *Agricultural and Forest
1456 Meteorology*, 123(1), 79-96. <https://doi.org/10.1016/j.agrformet.2003.10.004>
- 1457 Xu, Z., Shimizu, H., Ito, S., Yagasaki, Y., Zou, C., Zhou, G., & Zheng, Y. (2014). Effects of
1458 elevated CO₂, warming and precipitation change on plant growth, photosynthesis and
1459 peroxidation in dominant species from North China grassland. *Planta*, 239(2), 421-435.
1460 <https://doi.org/10.1007/s00425-013-1987-9>
- 1461 Yamori, W., Hikosaka, K., & Way, D. A. (2014). Temperature response of photosynthesis in C₃,
1462 C₄, and CAM plants: temperature acclimation and temperature

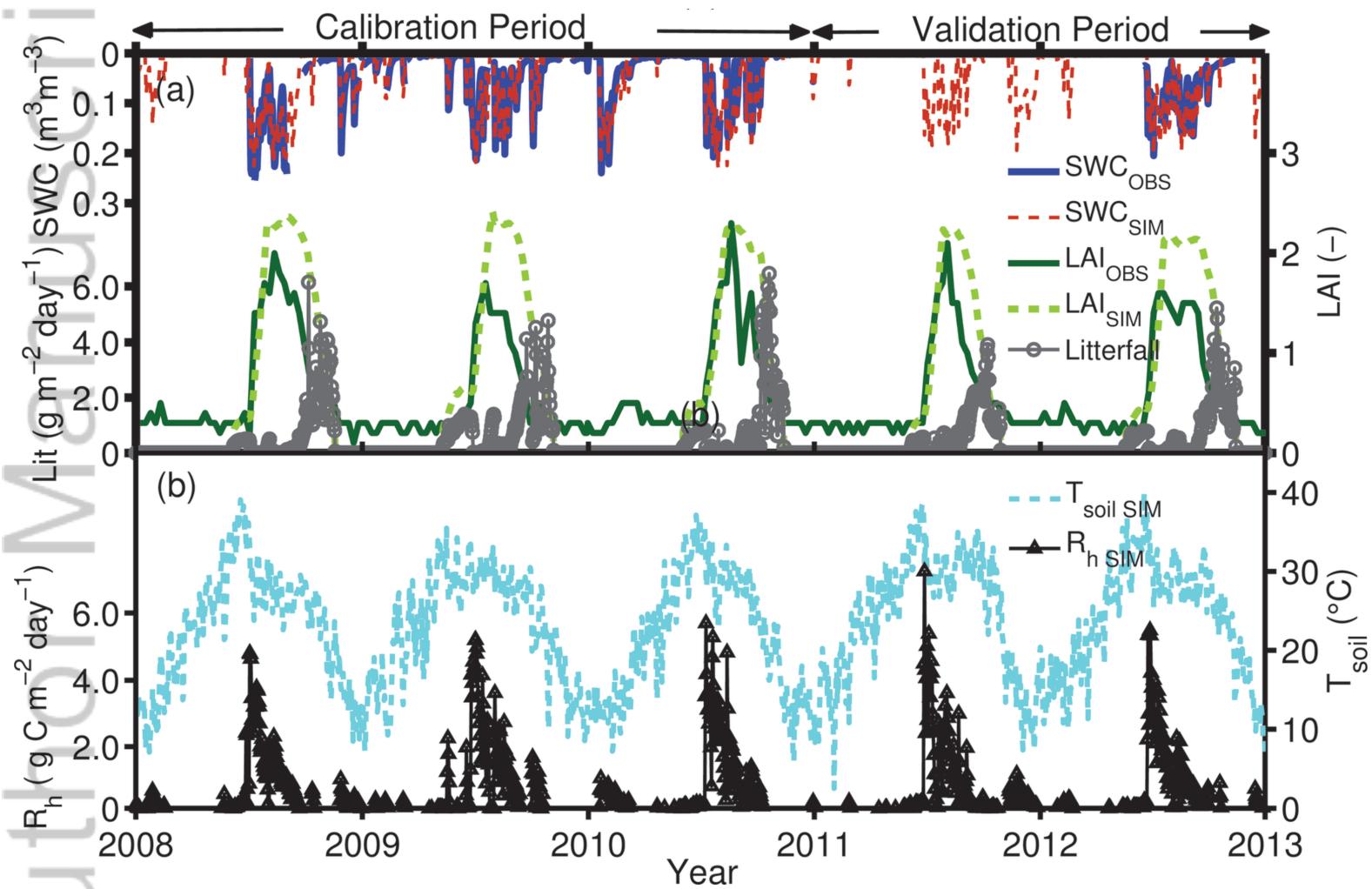
1463 adaptation. *Photosynthesis Research*, 119(1-2), 101-117.
1464 <https://doi.org/10.1007/s11120-013-9874-6>
1465 Yang, Y., Guan, H., Batelaan, O., McVicar, T. R., Long, D., Piao, S., ... & Simmons, C. T.
1466 (2016). Contrasting responses of water use efficiency to drought across global terrestrial
1467 ecosystems. *Scientific Reports*, 6, 23284. <https://doi.org/10.1038/srep23284>
1468 Yepez, E. A., Scott, R. L., Cable, W. L., & Williams, D. G. (2007). Intraseasonal variation in
1469 water and carbon dioxide flux components in a semiarid riparian
1470 woodland. *Ecosystems*, 10(7), 1100-1115. <https://doi.org/10.1007/s10021-007-9079-y>
1471 Zhang, X., Niu, G. Y., Elshall, A. S., Ye, M., Barron-Gafford, G. A., & Pavao-Zuckerman, M.
1472 (2014). Assessing five evolving microbial enzyme models against field measurements
1473 from a semiarid savannah—What are the mechanisms of soil respiration
1474 pulses?. *Geophysical Research Letters*, 41(18), 6428-6434.
1475 <https://doi.org/10.1002/2014GL061399>
1476 Zhou, X., Wan, S., & Luo, Y. (2007). Source components and interannual variability of soil CO₂
1477 efflux under experimental warming and clipping in a grassland ecosystem. *Global*
1478 *Change Biology*, 13(4), 761-775. <https://doi.org/10.1111/j.1365-2486.2007.01333.x>
1479 Zhou, Z., Jiang, L., Du, E., Hu, H., Li, Y., Chen, D., & Fang, J. (2013). Temperature and
1480 substrate availability regulate soil respiration in the tropical mountain rainforests, Hainan
1481 Island, China. *Journal of Plant Ecology*, 6(5), 325-334. <https://doi.org/10.1093/jpe/rtt034>
1482



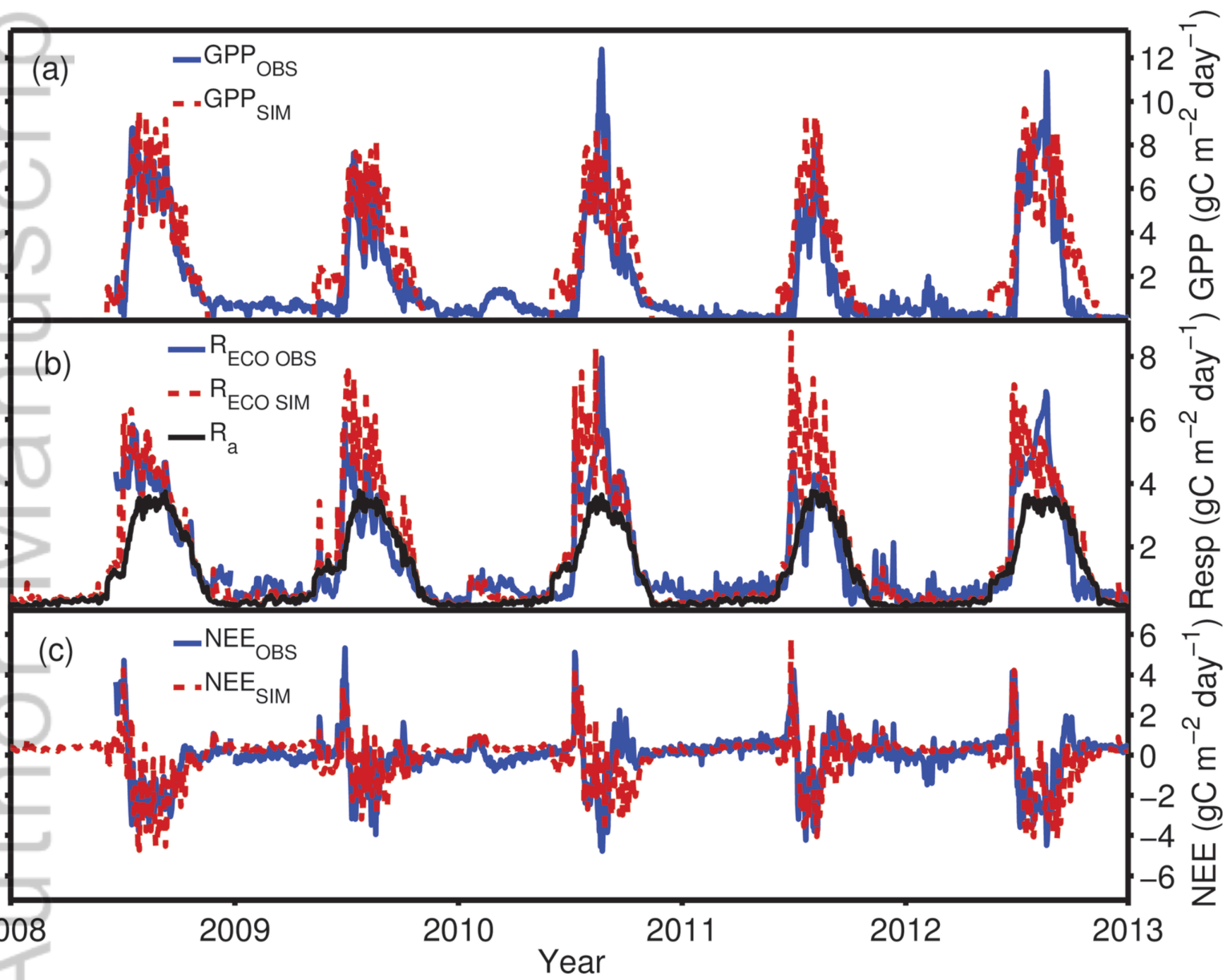
2017JG004361-f01-z-.tif



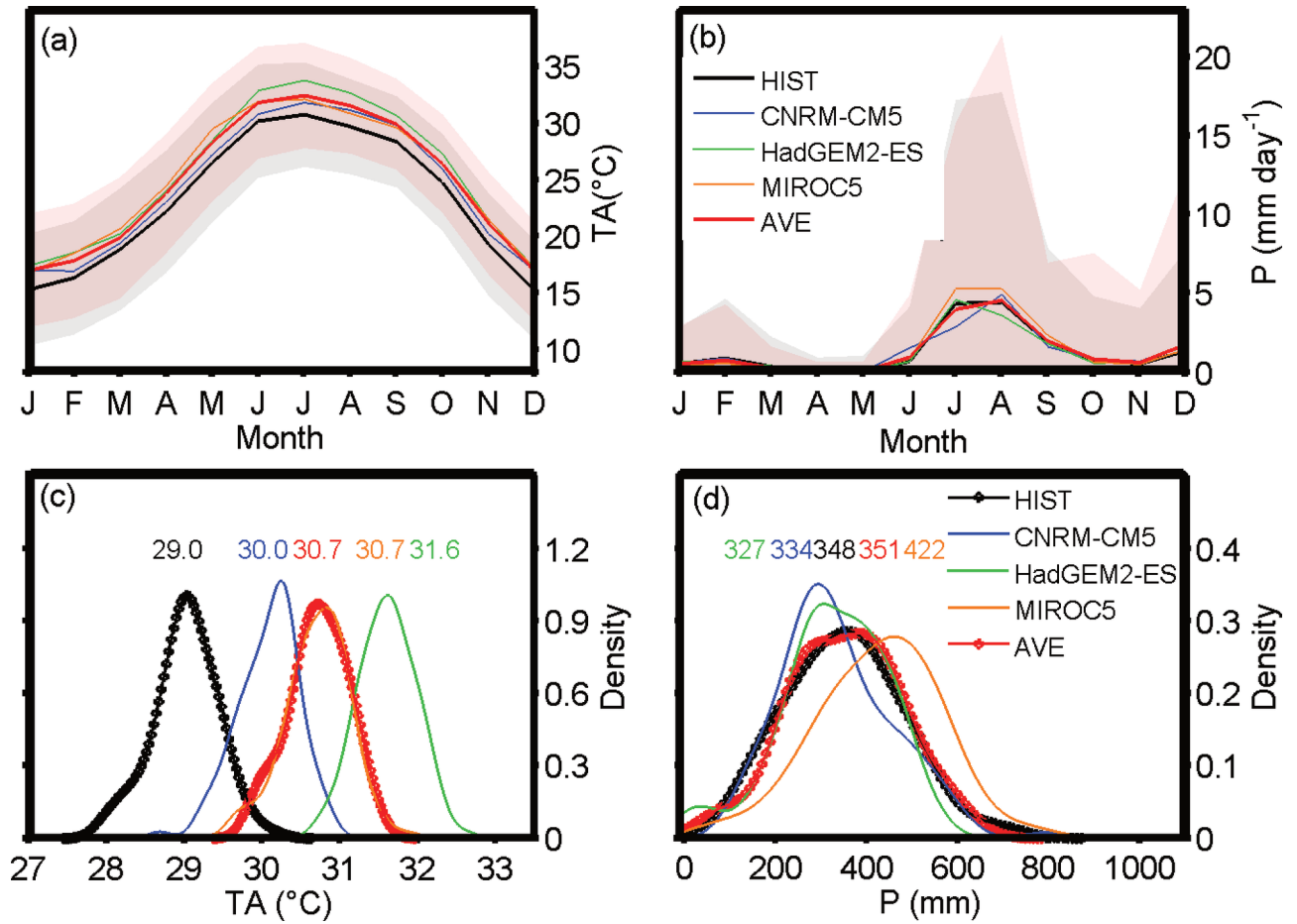




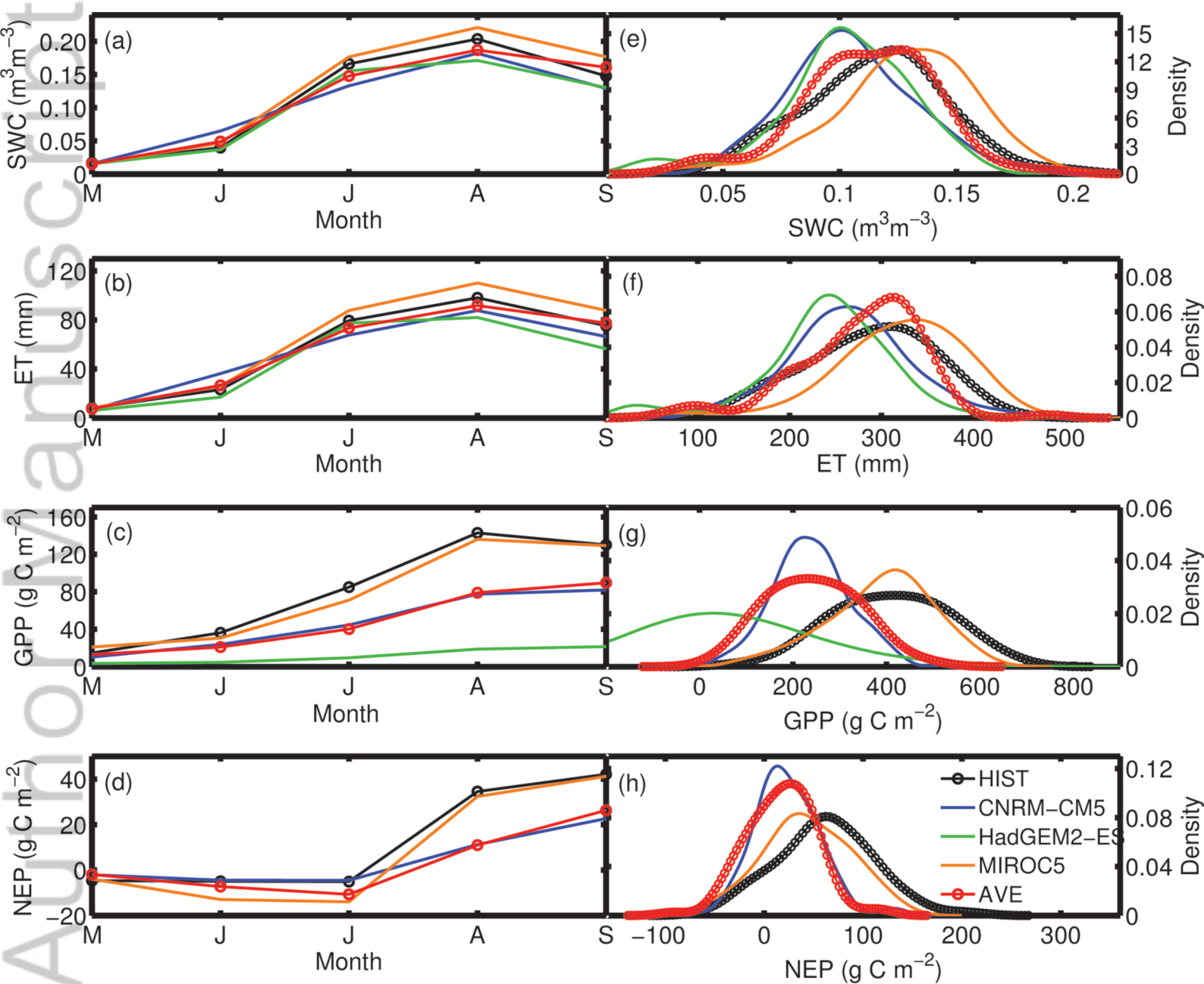
2017jg004361-f04-z-eps



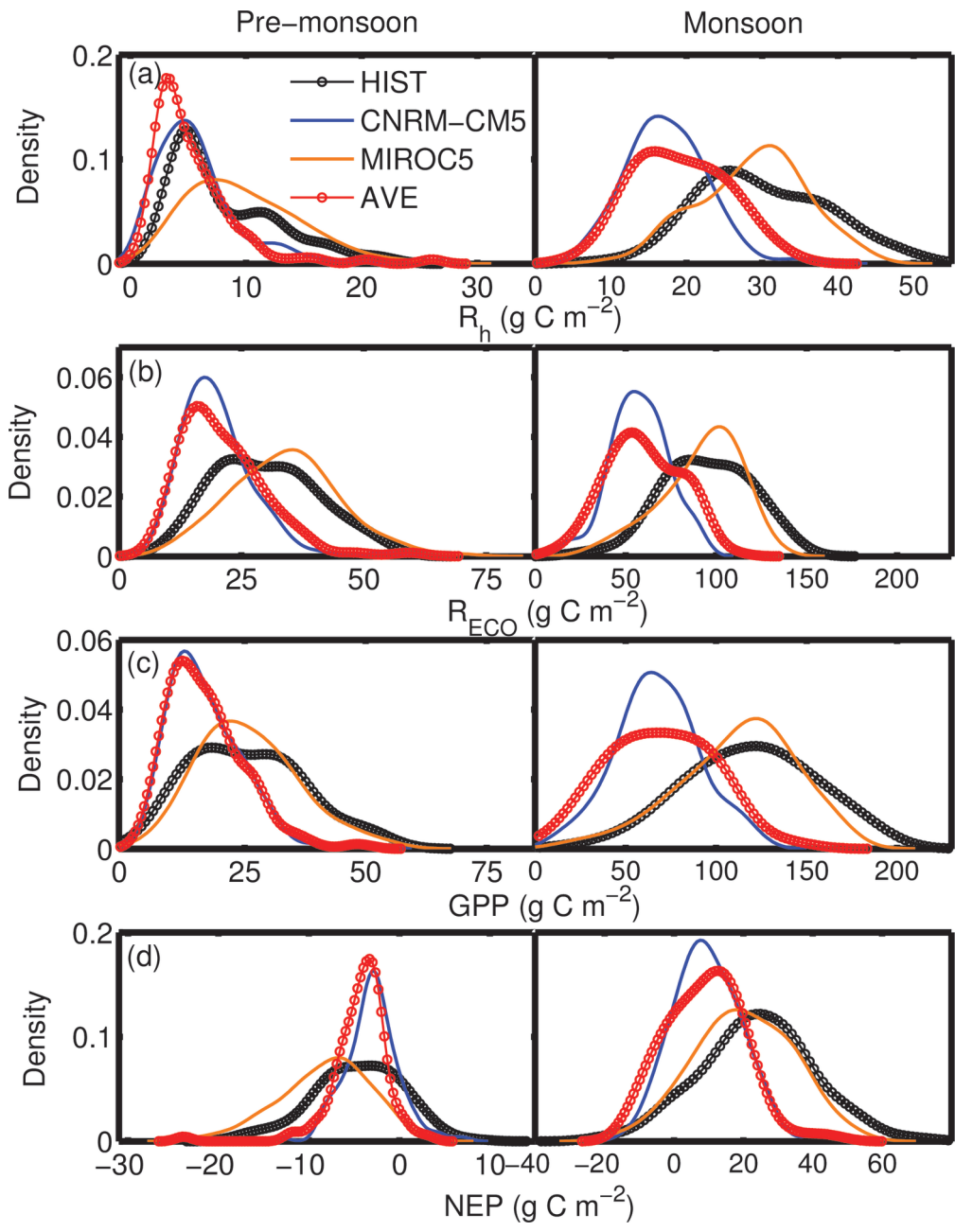
2017jg004361-f05-z-eps



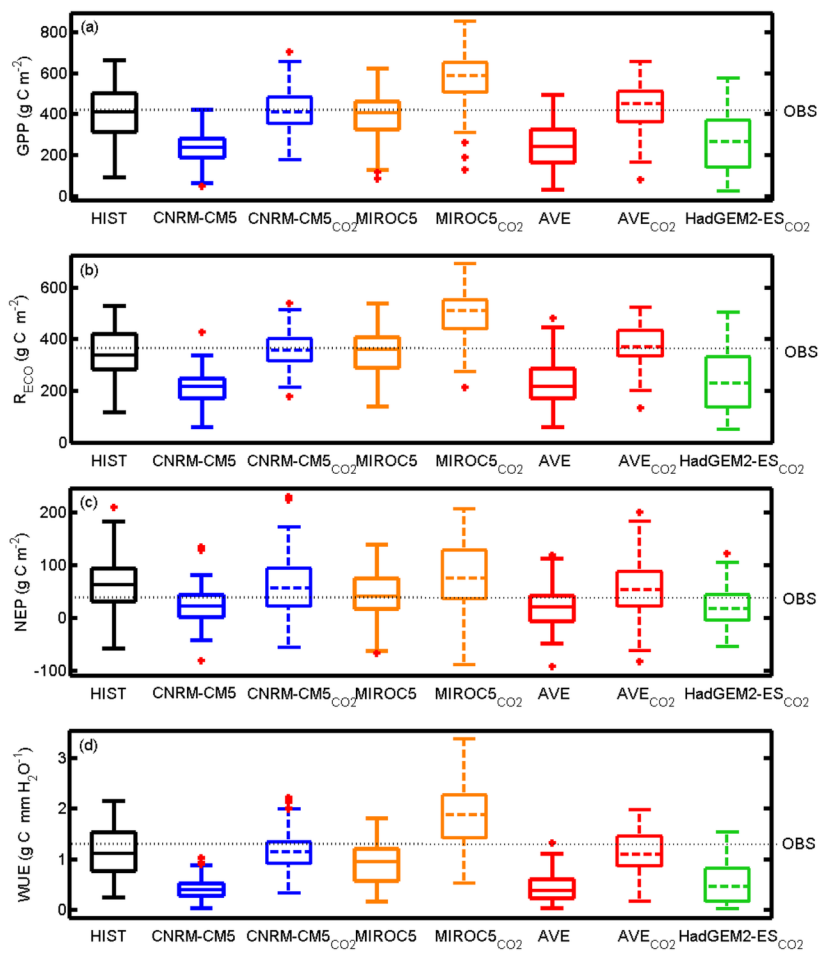
2017jg004361-f06-z-.eps



2017jg004361-f07-z-.eps



2017jg004361-f08-z-.eps



2017JG004361-f09-z-.tif